New Zealand Wind and Solar Generation Scenarios

26 April 2023

Executive summary

New Zealand is experiencing an increasing penetration of wind and solar generation due to the economic viability of these sources, in line with the government's aspiration of 100 percent renewable electricity by 2030. Such an increase brings challenges since wind and solar are variable energy sources and therefore cannot be dispatched according to demand, only according to the availability of the resource.

Variable electricity generation requires consideration about which and how much other energy sources are necessary to compensate for such variations (ie, provide firm generation). Since it is expected that variable renewable sources will make up an increasing proportion of total generation, it is crucial to understand the behaviour of these renewable sources to understand the scale of this firming requirement. Sufficient firming is critical for the transition to a low-emission electricity system to maintain the same level of reliability that we currently enjoy.

This paper models diversified renewable portfolios. By doing this we gain an understanding of the extent to which renewable generation firms itself. The remaining variation in renewable output is the scale of the firming required. It is worth noting that this study should not be interpreted as a feasibility study. Rather, it serves as an indication of the behaviour of solar and wind generation throughout New Zealand based on weather data available to the Authority. Thus, the wind and solar sites mentioned in the study were selected based solely on data availability (ie, existing weather stations); the technical feasibility or economic viability of the sites is completely out of the scope of the study.

Significant investment will be required to effect the transition to renewables. Concept Consulting Group Limited (Concept) estimated in 2021 that New Zealand could need investment of between $27 billion and $37 billion by 2050 to meet demand growth, replace thermal plant and maintain existing renewable generation[1]. However, as the winter 2023 consultation paper discussed[2], the increased role of intermittent (variable) renewables in the New Zealand electricity market may exacerbate reliability issues. This paper helps us to understand the implications of increased variable generation in the market. The modelling methodology equips us with the ability to provide on-going monitoring against expectations as new generation enters the market.

This study investigates expected generation profiles for potential wind and solar sites in NZ. Expected generation is modelled using weather data and assumptions for conversion of wind speed and solar irradiance to generation output. This is a simple model assuming standard wind turbines and solar panels. The results should be treated as a general indication of possible future generation trends from these sources.

The paper discusses the expected time profile of generation (daily and seasonal) and the spatial variability for wind and solar generation.

Two scenarios are analysed in this study. The first scenario models wind and solar sites for the entire country, using data from every location of MetService weather stations. The second selects the top-performing sites from the original set, discarding those located within Department of Conservation Te Papa Atawhai (DOC) protected areas.

If wind turbines were built at all 89 MetService weather station locations (scenario one), we estimate that wind generation would be below 10 percent of total capacity around 5 percent

[1]See: "Review of Generation Investment Environment." Concept Consulting. 2021. Available at: https://www.ea.govt.nz/documents/2164/Concept-Report_-Review-of-generation-investment-environment-v3.pdf.

[2]See: "Driving efficient solutions to promote consumer interests through winter 2023". Consultation paper. Electricity Authority Te Mana Hiko. 2022. Available at: https://www.ea.govt.nz/documents/1630/Driving_efficient_solutions_to_promote_consumer_interests_through_winter_2023.pdf

of the time. This would be an improvement on current performance – in 2022 16 percent of the time wind generation was lower than 10 percent of current installed capacity. Additionally, only around 9 percent of the time was our modelled generation above 50 percent of total capacity. The North Island sites performed better when compared to the South Island sites, generating above 50 percent of total capacity for 16 percent of the time (compared to 7 percent for the South Island sites).

We also found an increase in correlation between wind sites depending on their geographical proximity (the closer the sites, the higher the correlation). The wind sites showed an overall tendency to generate more energy during the daytime and during spring. During spring and summer, we found wind energy tends to peak around 4 pm while during winter it peaks around 2 pm. Wind generation had a greater daily variability in spring with a median daily variability of 79 MW, compared to 52 MW in winter. However, total wind generation in spring was 20 percent higher than in winter, on average.

For solar power, we estimate that generation would be below 10 percent of capacity around 60 percent of the time and above 50 percent of total capacity about 14 percent of the time. Like wind, the North Island outperformed the South, but by a smaller margin when compared to wind. The correlation between the solar sites remained high throughout the country, despite the increase in distance between the sites. Solar has a more pronounced daily variation compared to wind, which is expected due to the characteristics of this energy source. The median daily variation in summer was 126 MW, while in winter it was 80 MW. The average solar generation in summer was 47 percent higher when compared to winter.

Finally, regarding scenario two, the top performing wind sites showed higher capacity factors compared to scenario one (all sites) - 53 percent against 32 percent on average, respectively. The 13 top performing wind sites generated 25 percent of the total yearly generation of all 89 wind sites. For solar, on the other hand, and consistent with higher correlations between all solar sites, the capacity factors were similar (around 20 percent on average).

Contents

1 Introduction

1.1. New Zealand is experiencing an increasing penetration of wind and solar generation due to the economic viability of these sources. Moreover, such an increase is aligned with the government's aspiration of 100 percent renewable electricity by 2030. Since it is expected that variable renewable sources will make up an increasing proportion of total generation, it is crucial to understand the behaviour of these renewable sources.

1.2. This study investigates the expected generation duration for the wind and solar sources whilst also discussing their time and spatial variability using seven years of data. The study is based on the availability of in-loco solar irradiance and wind speed data measured by the MetService weather stations. The location of the theoretical wind and solar sites is set to the locations of the weather stations providing data for this analysis. The study simulates the performance of a single wind turbine with a nominal capacity of 3 MW and a solar photovoltaic (PV) array designed to provide the same nominal capacity.

1.3. It is worth mentioning that this study should not be interpreted as a feasibility study. This study serves as an indication of the behaviour of solar and wind generation throughout New Zealand based on weather data available to the Authority. When looking at tecno-economical aspects, site-specific variables should be included in the analysis, which is out of the scope of this study.

1.4. The simulation accounts for both the change in air density due to variations in air temperature and air pressure, as well as correcting the wind speed according to turbine hub height (assuming that wind data is measured at a height of 10 m above ground). Wind gusts, wind direction, and site elevation information are not accounted for at this stage of the study. Solar irradiance was adjusted to reflect the irradiance at the plane of the solar PV array since the available data is measured parallel to the ground.

1.5. The analysis also discusses the time (both daily and seasonal) and space variability of renewable sources (wind and solar).

2. Methodology

Wind and solar data from local weather stations

2.1. The study uses 7 years of data ranging from 01 January 2015 to 31 December 2021, recorded hourly. The interval was chosen because (1) the number of wind farms operating in New Zealand remained constant during this period[3], and (2) both La Niña and El Niño events occurred during this period. The study modelled 89 wind sites (one turbine per site) and 61 solar sites. The location of the sites corresponds to the weather stations where the solar and/or wind data were available.

2.2. A process of cleaning and preparing the data set removed inconsistent values from the set. The study excludes any wind speed values above 50 m/s since it is typically

[3] See: "Wind Energy." International Renewable Energy Agency. 2022. Available at: https://www.irena.org/Energy-Transition/Technology/Wind-energy.

above the threshold that most wind turbines are designed to operate. We did not identify any negative wind speed or solar irradiation data in the data set. A few high solar irradiation values (above 1,360 W/m^2 – solar irradiance at the top of the atmosphere) were identified but were not removed since they can be due to lensing effects.

2.3. No investigation was performed on the quality of the weather data; this study assumes that the information is correctly acquired, processed, and maintained by the organisation that makes the weather database available.

How we modelled wind power

2.4. The available wind power (P_w) is a function of the air density (ρ), the cross-sectional area exposed to the wind (A), and the cube of wind speed (v), as follows:

$$P_w = 0.5 \cdot \rho \cdot A \cdot v^3 \qquad (1)$$

2.5. The following subsections describe the process of computing the available wind power and the theoretical power generated by the wind turbines.

Adjustments and assumptions of the model

2.6. The air density (ρ) was calculated for each hour value based on the ideal gas law, using air temperature and air pressure values, as follows[4]:

$$\rho = \frac{P_a}{(R \cdot T)} \qquad (2)$$

2.7. Where P_a represents air pressure (in Pascals), R represents the universal gas constant, and T represents the temperature (in Kelvin). Wind speed values, originally recorded in knots, were converted to metres per second by a conversion factor ($1\ m/s\ =\ 0.5144\ knots$). The wind speed at the hub height (v_{90}) was adjusted according to the logarithmic law

$$v_{90} = v_0 \frac{ln(h_2/z_0)}{ln(h_1/z_0)} \qquad (3)$$

2.8. where v_{90} refers to the wind speed at the wind turbine hub height (90 m above ground); h_2 represents the hub height; h_1 represents the measurement height (assumed as 10 m above ground); z_0 represents the roughness of the terrain (assumed to be 0.1)[5].

Turbine Performance

2.9. This study models site performance based on the Vestas V112 wind turbine, since it is a relatively modern turbine that can work on a wide range of wind speeds, as

---

[4] See: Carl R. Nave. 2019. “Ideal Gas Law”. HyperPhysics. Georgia State University Available at: http://hyperphysics.phy-astr.gsu.edu/hbase/Kinetic/idegas.html

[5] See: Anjum, Lalit. "Wind resource estimation techniques-an overview." *Int. J. Wind Renew. Energy* 3, no. 2 (2014): 26-38.

shown in Figure 1. The turbine is designed to achieve its nominal capacity of 3000 kW at or above wind speeds of 15.5 m/s (and lower than its cut-off threshold of 25 m/s). It has a swept area (A) of 9852 m^2 and operates according to the power curve shown below

Figure 1 - Vestas V112 Power Curve. Source: The WindPower[6]

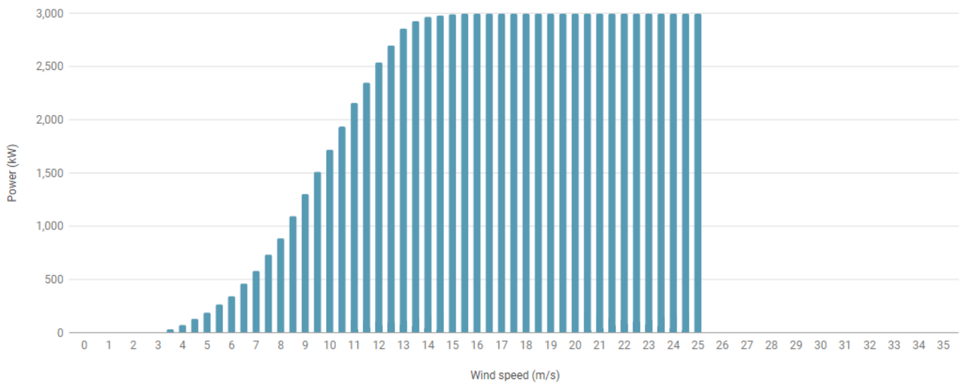

2.10. As shown in Figure 1 values below 3.5 m/s and above 25 m/s are below the cut-in or above the cut-off speed, where the turbine does not generate power. The area between 15.5 m/s and 25 m/s represents the wind speed values where the turbine operates at its nominal capacity (3,000 kW). Finally, the area between 3.5 m/s and 15.5 m/s follows equation 4 ($R^2 = 0.9997$) below, which uses wind speed at the hub height as its main input:

$$P_{W,V112} = -2.0189 \cdot {v_{90}}^4 + 52.09 \cdot {v_{90}}^3 - 432.94 \cdot {v_{90}}^2 + 1606.7 \cdot v_{90} - 2128.2. \quad (4)$$

How we modelled solar power

2.11. The solar irradiation was converted into solar energy by making use of the PVLib open-source tool developed by the Sandia Laboratory PV Performance Modeling Collaborative[7]. The tool provides a set of functions designed to simulate the performance of solar photovoltaic (PV) systems based on solar irradiance and other weather and locational inputs.

2.12. The modelled solar PV system is composed of 8,800 solar PV modules (REC Solar – REC380TP2SN 72) and 50 solar inverters (ABB TRIO-TM-60.0-US-480). With such configuration, the system DC to AC ratio is estimated to be 1.11 and it can deliver 3,000.00 kWac of nominal capacity, thus matching the nominal capacity of the wind generator. Note that the total DC nameplate capacity is higher, 3,344.25 kWdc but since solar PV modules degrade over time (around 0.5 percent per year), having a DC/AC ratio above 1 ensures that the system will deliver the rated AC capacity for most of the lifetime of the project.

[6] See: "Vestas V112/3000 - Manufacturers and Turbines - Online Access". The Wind Power – Wind Market Intelligence. 2022. Available at: https://www.thewindpower.net/turbine_en_413_vestas_v112-3000.php.

[7] See: Anderson, K., Hansen, C., Holmgren, W., Jensen, A., Mikofski, M., and Driesse, A. "pvlib python: 2023 project update." Journal of Open Source Software, 8(92), 5994, (2023). Available at: https://pvpmc.sandia.gov/tools/pv_lib-toolbox/ .

2.13. The modelled solar PV system was assumed to have 20 degrees tilt relative to the horizon (PV array tilt angle), facing North (0 degrees of azimuth). To perform the simulation, PVLib requires information on the global horizontal irradiance (GHI), global diffuse irradiance (DHI), and direct normal irradiance (DNI). The data is used to calculate the total irradiance received at the plane of the array (POA). In the case of this study, the DNI and DHI were derived from the GHI, since it was the only solar information available. The DNI was calculated using PVLib *dirint* method, which uses a modified DISC (Dynamic Global-to-Direct Irradiance Conversion) model developed by Perez et al (1992)[8]. The DHI was calculated using the following relationship:

$$GHI = DNI \cdot cos(\theta_z) + DHI, \tag{5}$$

2.14. where θ_z represents the solar zenith angle, which is also calculated by PVLib based on the time of the day and the location of the solar PV system and adjusted using weather variables such as air temperature and pressure. When appropriate, the solar zenith angle was also used to remove night-time values (values above 85 degrees) from the data set. Solar irradiance units are in W/m^2.

How we calculated the correlation between sites

2.15. In this study, we calculated the correlation coefficient between locations to investigate the strength of association between any two sites. The study analyses one technology at a time (ie, wind sites are compared to wind sites only). Positive coefficient values indicate that generation should follow a similar trend at both sites (eg, an increase in generation at one site would correspond to an increase in generation at the other site). Negative values would then indicate an inverse response between sites.

2.16. This study calculates the correlation between the performance of the modelled wind and solar farms using the Pearson[9] correlation method. The method assigns values between -1 and 1 to the results; the greater the value, the more positively correlated the variables are. Negative values indicate that the values are negatively correlated. Values at or close to zero indicate no correlation. Typically, values above +/- 0.7 indicate a strong correlation[10].

3. Results

Wind generation only reaches above 50 percent of installed capacity around 9 percent of the time

3.1. Figure 2 shows the wind generation duration curve (GDC) for the entire analysis period (2015-2021, sampled hourly). The figure shows that approximately 5 percent of the wind power was below 27 MW (10 percent of total capacity) during the period.

---

[8] See: Ineichen, Pierre, R. R. Perez, R. D. Seal, E. L. Maxwell, and A. J. A. T. Zalenka. "Dynamic global-to-direct irradiance conversion models." *Ashrae Trans* 98, no. 1 (1992): 354-369.

[9] We compared Spearman's rank correlation against Pearson and found differences to be in the order of 10^{-2}

[10] See: Nettleton, D., 2014. "Pearson Correlation - an Overview." Science Direct. 2014. Available at: https://www.sciencedirect.com/topics/computer-science/pearson-correlation.

3.2. This gives a sense of the firming that would be required for a diversified wind portfolio. About 5 percent of the time, firming would be required for 90 percent of the installed wind capacity — assuming that demand was sufficient to support this generation. Below the paper explores the seasonal and intraday behaviour of wind and solar.

3.3. Figure 2 also shows that only around 9 percent of the time generation was above 135 MW (50 percent of total capacity with 3MW at 89 sites). Appendix 4 shows the frequency that the modelled wind speed data fell below the turbine cut-in and cut-off speeds, for each of the sites considered in this study.

Figure 2 – Wind generation duration curve for the entire set of modelled wind sites

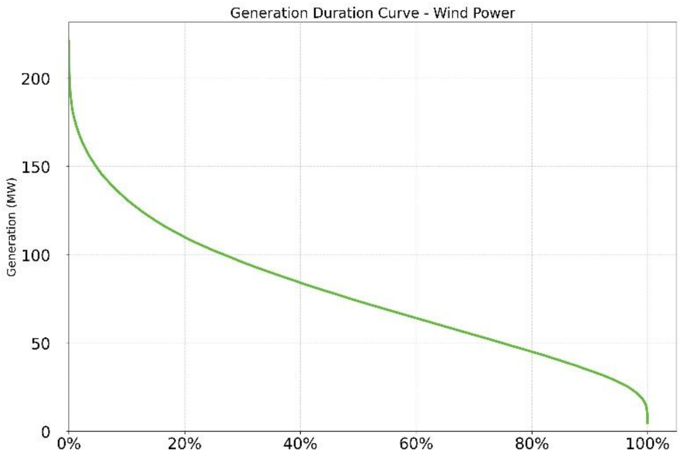

Solar generation is below 10 percent of total capacity more frequently than wind, even excluding night-time

3.4. The solar GDC (Figure 3) shows a different pattern when compared to wind, for the same period (2015-2021). Solar generation happened only approximately 50 percent of the time during the period. Such a difference is due to the presence of night-time values and is therefore expected (since solar generation cannot happen during the night)[11]. Figure 3 shows that 60 percent of the time solar generation is below 20MW (10 percent of capacity with 3MW at 61 sites). Approximately 14 percent of the time generation was above 91.5 MW (50 percent of total capacity).

3.5. Considering only the daytime values, 20 percent of the time generation would be below 10 percent of total capacity and 28 percent of the time above 50 percent of total capacity, for the same period.

3.6. The implications for firming for wind and solar are similar. Below the paper explores the seasonal and intraday behaviour of wind and solar.

[11] Although solar photovoltaics can generate power only during daytime, it is relevant to analyse the resource on a 24-hour basis to facilitate the comparison of the result against other technologies or against demand. Moreover, capacity factors are usually calculated on 24-hour basis independent of the technology.

Figure 3 – Solar generation duration curve for the entire set of modelled solar sites

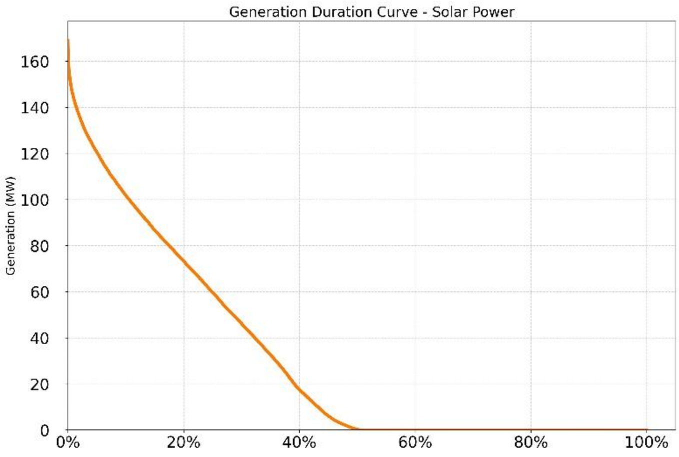

Wind generation is highest in spring and solar in summer

3.7. Figure 4 and Figure 5 show the wind and solar generation behaviour according to the season of the year for the period of study (2015-2021). The main difference between the two generation sources is that wind power shows higher values during the Spring season (average of 87.9 MW, or 33 percent of total capacity), while solar power reaches its peak in Summer (average of 71.6 MW, or 39 percent of total capacity). Wind generation during Spring showed an average of 192 GWh, or 28 percent of average annual generation. Solar shows a summer average of 91.8 GWh, or 34 percent of average annual generation. In general terms, though, both variables are expected to show higher values during warmer seasons (Spring and Summer).

3.8. This suggests that the greater firming would be required in winter when demand is highest and both wind and solar generation are lowest.

Figure 4 - Wind power frequency histograms relative to the season of the year

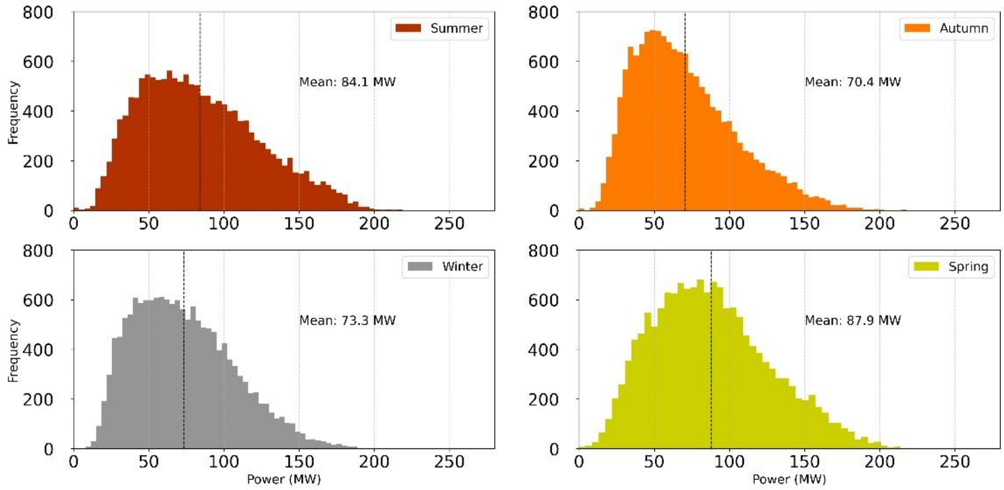

3.9. It is also interesting to note that solar power is more heavily affected by seasonal variations when compared to wind. For instance, whilst wind shows a 17.5 MW difference between Spring and Autumn (ie, the difference between the highest and lowest seasonal wind power average values), solar exhibits a 23 MW difference between its Summer and Winter average values. This analysis excludes night-time values.

Figure 5 - Solar power frequency histograms relative to the season of the year

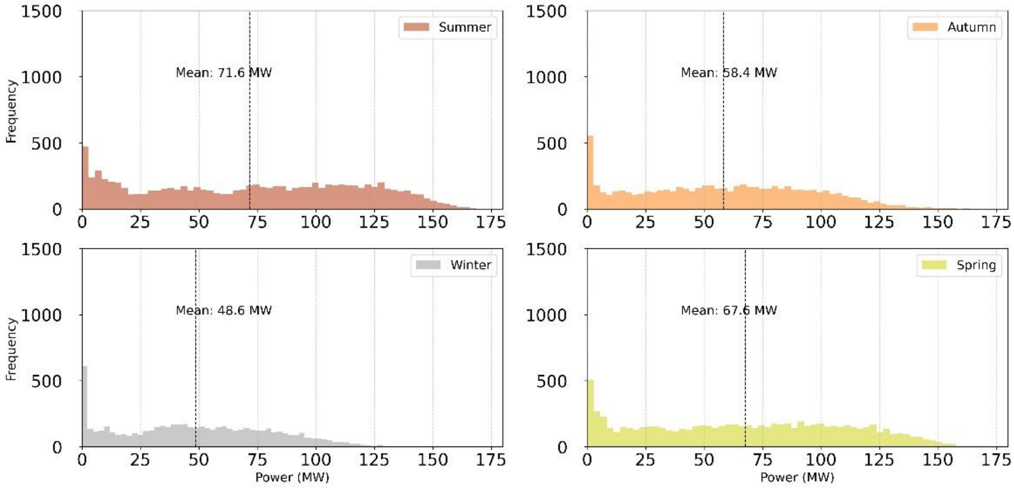

3.10. The wind speed and solar global horizontal irradiance (GHI) histograms can be found in Appendix 1.

Both wind and solar show daytime peaks but wind generation peaks later in the day

3.11. The original seven years of data (2015-2021) were grouped into a single averaged year consisting of hourly values for all the wind and solar sites, to show the daily generation pattern. The results are shown in Figure 6 and Figure 8 in the form of box-and-whiskers graphs, for June and December. Note that since these are averaged values, the variability for any individual day could be higher than these charts show, as shown in Figure 7 and Figure 9. For example, the maximum daily variability for wind generation occurred on 19 December 2017, from a low of 34 MW at 3 am to 187 MW at 4 pm.

3.12. Wind and solar show an increase in generation during the daytime (as expected for solar). However, whilst solar reaches its peak around 1 pm, wind peaks later, between 3 and 5 pm. The seasonal effect can also be noted in the graphs, as June shows lower wind and solar generation values relative to the total capacity, compared to December. There is also greater variability over a day in December compared to a day in June.

3.13. That peak renewable generation occurs off-peak, it is less likely to contribute to peak demand and increases the requirement for firming.

3.14. Figure 7 further illustrates the daily variability in wind generation. It shows that over 2015 to 2021, the median daily variability was 79 MW for spring compared to 52 MW in winter. The daily variability in spring is lower compared to summer, which showed 82 MW of median variability. In other words, despite being the second-best season for wind generation in terms of total electricity generated, summer shows a slightly higher variability when compared to spring.

Figure 6 - Boxplot of the hourly wind power generation for the months of June and December

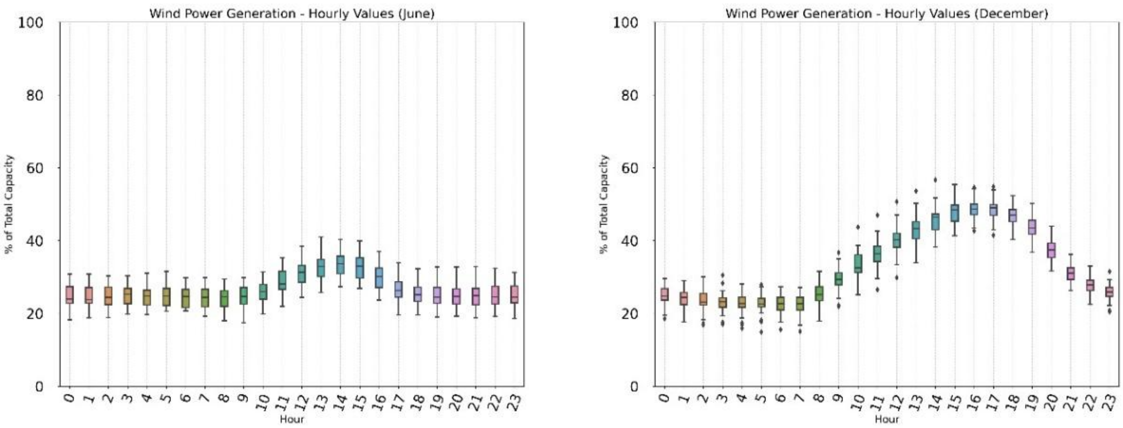

Figure 7 – Daily variability of wind generation by season

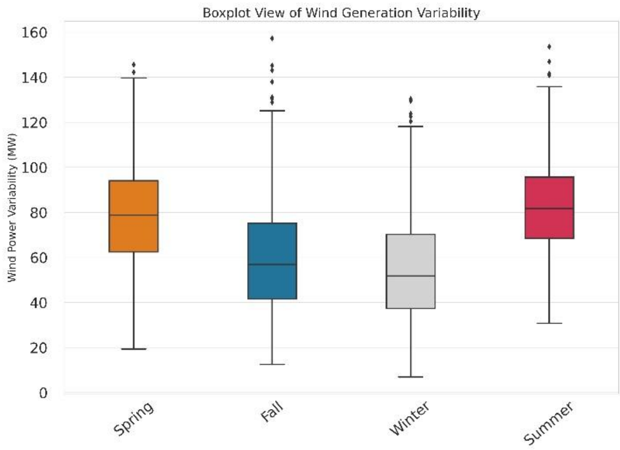

3.15. Figure 8 shows the response of the modelled solar sites during operational hours for the months of June and December (averaged over all years). As expected, the early morning and late afternoon values are lower when compared to the middle of the day, when the solar zenith angle is close to its lowest. Therefore, a solar PV system would be expected to generate most of its energy between 11 am and 3 pm during the winter and between 9 am and 6 pm in Summer. Figure 9 shows that over 2015 to 2021, the median daily solar variability was 126 MW in summer compared to 80 MW in winter. In this case summer showed the highest average generation values as well as higher daily variability. The charts for the remaining months can be found in Appendix 2.

Figure 8 - Boxplot of the hourly solar energy generation for the months of June and December

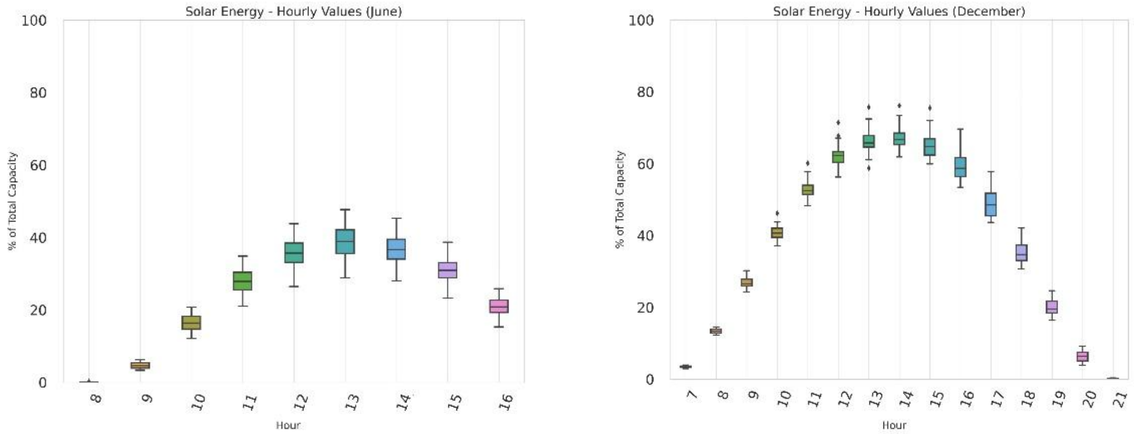

Figure 9 – Daily variability of solar generation by season

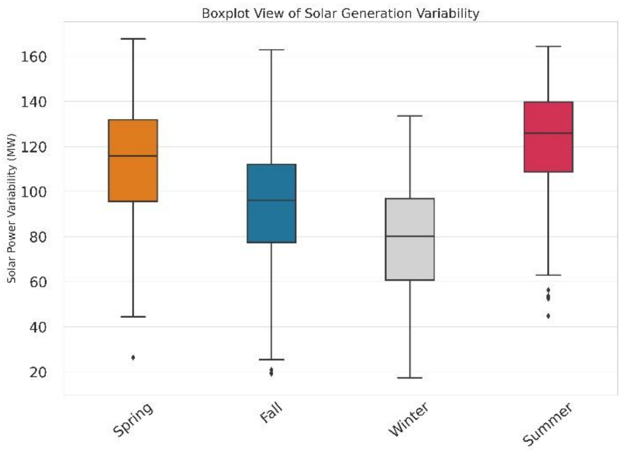

Geographical location affects wind generation more than solar

3.16. Up to this point, this study focused on analysing wind and solar generation through different time intervals. In this section, the focus changes to the analysis of the spatial variation of generation, investigating how generation differs for the North and South Islands and between regions (inter and intra-regional variation). To complete the task, the country was divided into 17 regions, following the New Zealand regional council boundaries[12] as shown in Figure 10.

[12] Data source: "Regional Council 2020 (generalised)." Stats NZ Geographic Data Service. Stats NZ Tatauranga Aotearoa. 2020. Available at: https://datafinder.stats.govt.nz/layer/104254-regional-council-2020-generalised/

Figure 10 – Map showing the location of weather stations whose data served as the basis for modelling wind or solar output (blue and orange dots, respectively). The coloured areas represent a region of the country. Note that some stations provide both solar and wind information

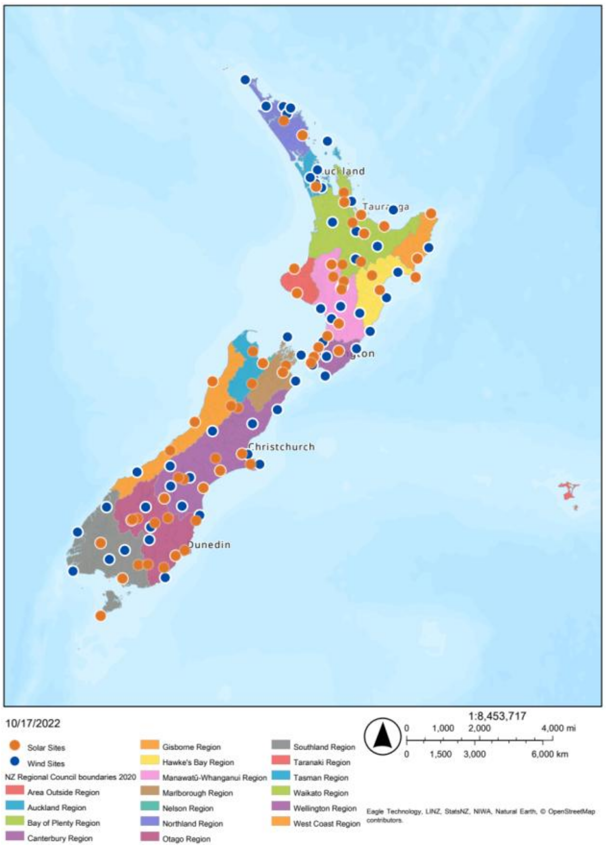

The North Island performed better by a small margin

3.17. Figure 11 shows the wind generation duration curve (GDC) for the North and South Islands for the 2015-2021 period. The difference between generation values in the two islands is related to the fact that there are 55 sites in the North Island, compared to 34 sites in the South. For the North Island, 5 percent of the time generation is below 10 percent of the total capacity, whilst for the South Island, 13 percent of the time generation is below the 10 percent capacity mark. 16 percent and 7 percent of the time generation is above the 50 percent level for the North and South Islands respectively, showing that the North Island modelled results performed better than the South Island.

Figure 11 – Wind GDC for the North (left chart) and South Islands (right)

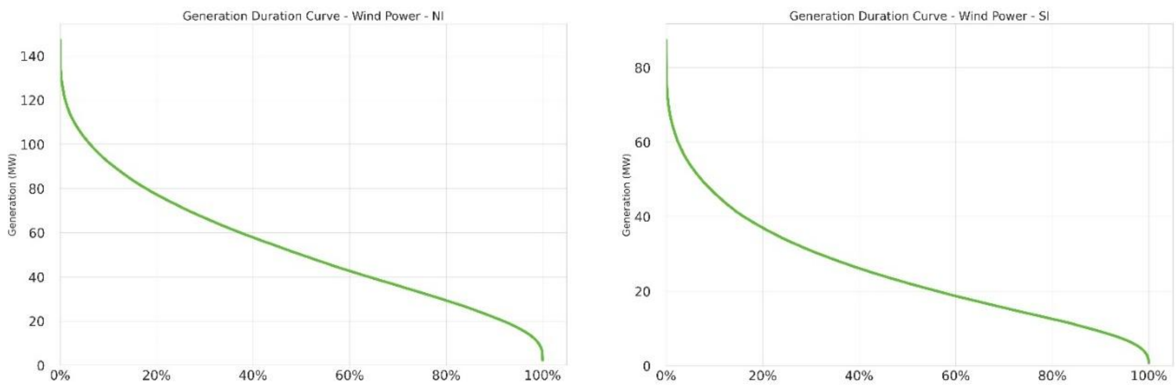

3.18. Figure 12 shows the solar GDC for the North and South Islands for the 2015-2021 period. In this case, the number of sites is similar: 29 sites in the North Island versus 32 in the South. For solar, the North and South Islands had similar percentages of low generation (59 percent and 60 percent of the time, respectively, generation was below 10 percent of total capacity). However, the North Island performed slightly better for higher amounts of generation, with generation above 50 percent of total capacity 15 percent of the time, compared to 12 percent of the time in the South Island. This slightly better performance is expected since the North Island is closer to the Equator. This analysis includes night-time values.

Figure 12 – Solar GDC for the North (left chart) and South Islands (right)

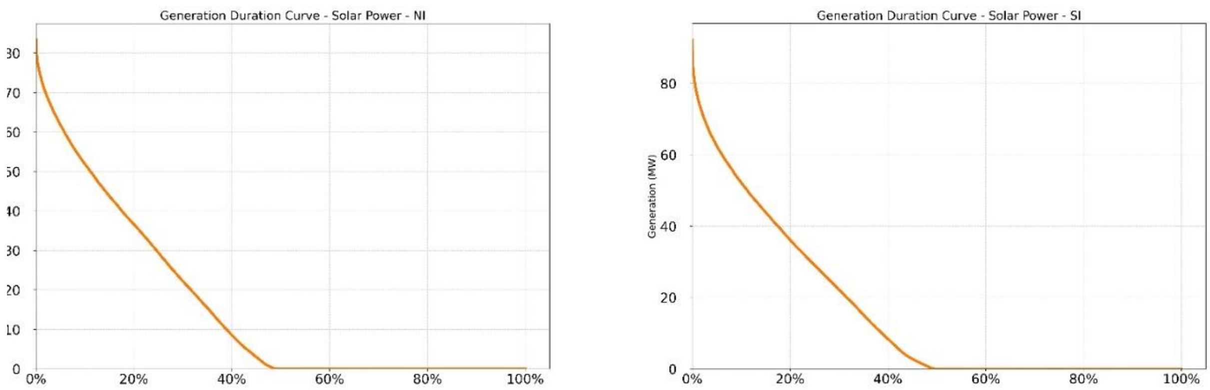

Wind varies more within regions

3.19. The intra-regional analysis showed that the performance of wind sites within a region can vary significantly as illustrated by Figure 13. Figure 13 and Figure 14 show the performance statistics (box-and-whisker charts) and correlation analysis for the wind and solar sites located in the Wellington region.

Figure 13 – Left: box-and-whisker chart showing the modelled performance of the wind farms in the Wellington region. Right: Correlation between sites.

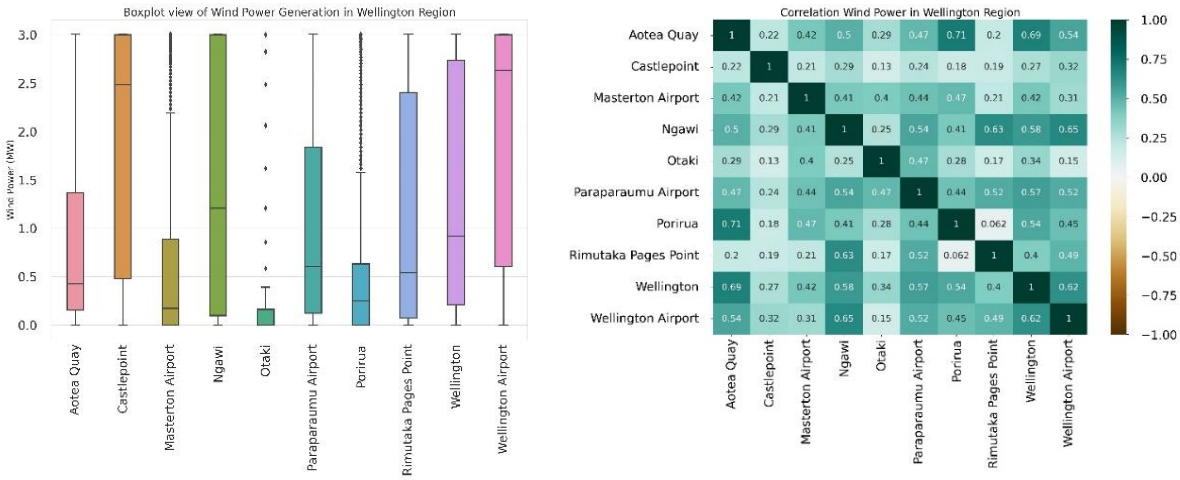

3.20. Figure 13 shows that the performance of the 10 wind sites modelled in the Wellington region vary considerably, with places such as Castlepoint and Wellington Airport showing better results compared to the other sites. For wind, correlation also varies depending on the distance between sites, decreasing with the increase in geographical distance. In the case of solar, the performance of the sites tends to be more similar, as shown in Figure 14. Both the intra-regional variability and the inter-regional variability are lower compared to wind. The lowest correlation between solar sites in the Wellington region was 0.68, compared to 0.13 for wind.

Figure 14 - Left: box-and-whisker chart showing the modelled performance of the solar arrays modelled for the Wellington region. Right: Correlation between sites

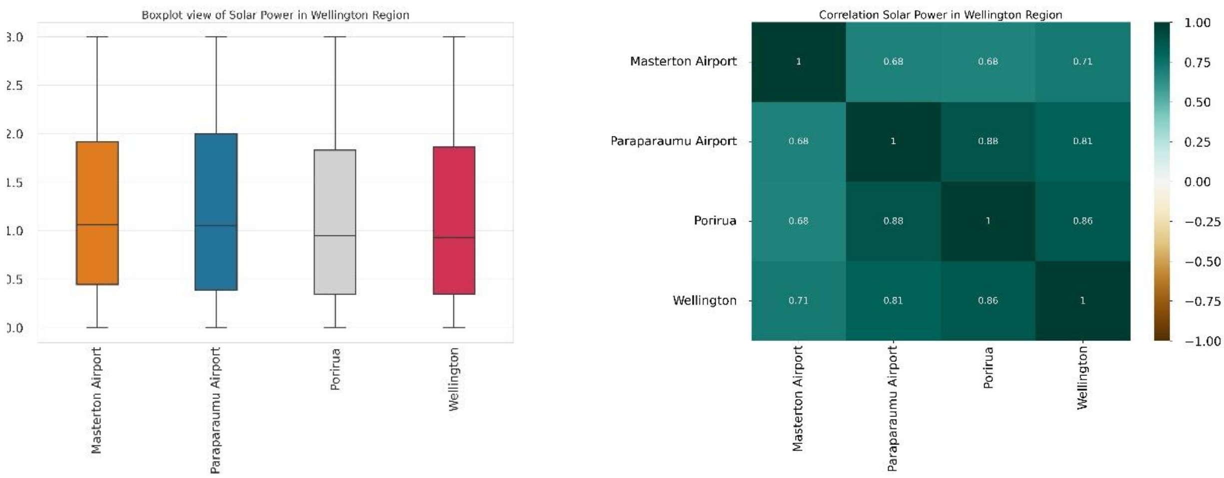

3.21. The pattern repeats for the remaining regions, where wind shows a higher intra-regional variability, in terms of performance, and lower intra-regional correlations compared to solar. The results obtained for the remaining regions can be found in Appendix 3.

3.22. The inter-regional analysis shows that wind varies even more between regions but solar remains highly correlated. For the inter-regional analysis, we selected the top-performing sites in each region. Sites located within protected areas defined by the DOC[13] were excluded from the analysis.

3.23. Figure 15 shows the correlation analysis for 13 selected wind sites. We found that the inter-regional correlations are lower when compared to the intra-regional correlations, again showing the decrease in correlation the greater the geographical distance between sites. As an example, the correlation between Cape Reinga and Whangaparaoa sites is higher compared to the correlation between the Cape Reinga and Le Bons Bay sites (0.57 and 0.049 respectively).

Figure 15 - Correlation between the selected wind sites. Note that the inter-regional correlation for wind is lower when compared to intra-regional values

3.24. Figure 16 presents the solar inter-regional analysis for 15 sites. The figure shows a different result compared to wind, as regional differences do not seem to affect the correlation, which remains relatively high across sites. In other words, solar power sites show a positive correlation across the country. This is somewhat expected since New Zealand is relatively 'narrow' in terms of longitude, thus the country will exhibit similar day and night patterns (in terms of solar time).

[13] Data source: "Protected Areas" Land Information New Zealand via LINZ Data Service. Toitū Te Whenua Land Information New Zealand. 2020. Available at: https://data.linz.govt.nz/layer/53564-protected-areas/.

Figure 16 - Correlation between the selected solar sites. Note that inter-regional correlation between the solar sites did not show to decrease with the increase in distance between sites

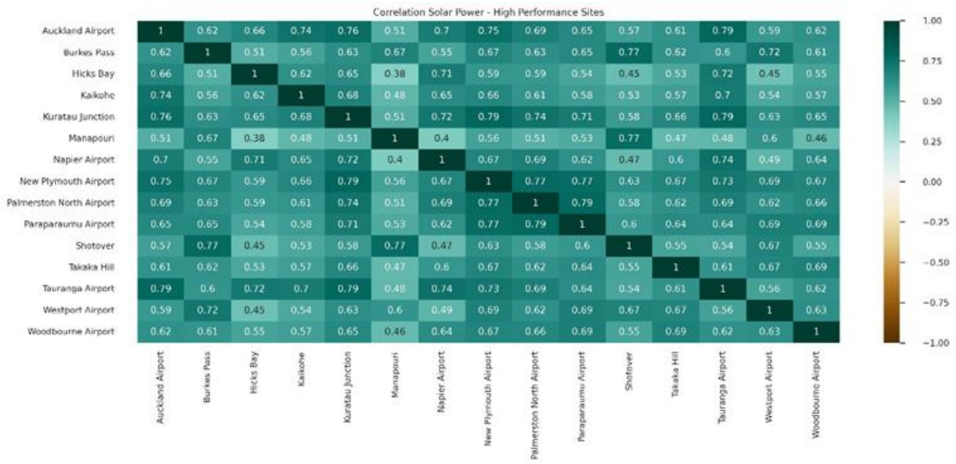

Capacity factors are higher for the top performing wind sites

3.25. This section presents the analysis of the average annual wind and solar generation and their respective capacity factors. Table 1 shows the results for wind, where, despite the higher annual energy values when considering all wind sites, the capacity factors are lower when compared to the top performing sites. It can also be inferred from the table that the 13 selected sites are responsible for almost 25 percent of the yearly generation from all 89 sites.

Table 1 - Average wind generation and capacity factors for the scenarios assessed in the study: all 89 wind sites versus 13 selected sites

	All Sites		Selected Sites	
Year	**Average Wind Gen (GWh)**	**Average Capacity Factor**	**Average Wind Gen (GWh)**	**Average Capacity Factor**
2015	684.9	32.8%	169.9	54.6%
2016	666.3	32.2%	154.1	52.4%
2017	646.8	30.9%	155.3	52.3%
2018	686.1	30.6%	173.8	52.1%
2019	756.9	33.0%	181.1	53.9%
2020	720.1	31.9%	167.8	52.7%
2021	681.3	30.6%	162.6	52.4%

3.26. Table 2 presents the analysis compiled for the solar sites. Despite the 15 selected sites being the better performing sites, the capacity factors do not increase considerably. This is consistent with the high correlations between solar sites presented in the previous section. The table also presents a comparison of the average capacity factor values, including and excluding night-time values (represented by the cases when the solar zenith angle is lower than 85 degrees - $\theta_z < 85°$).

Table 2 - Average solar generation and capacity factors for the scenarios assessed in the study: all 61 solar sites versus 15 selected sites

	All Sites			Selected Sites		
Year	Average Solar Gen (GWh)	Average Capacity Factor	Average Capacity Factor (θ_z< 85º)	Average Solar Gen (GWh)	Average Capacity Factor	Average Capacity Factor (θ_z< 85º)
2015	268.8	19.1%	41.5%	73.7	20.3%	44.1%
2016	254.4	18.1%	39.3%	70.1	19.2%	41.7%
2017	271.6	18.1%	39.4%	73.6	19.7%	42.6%
2018	273.4	18.0%	39.1%	75.1	19.4%	42.0%
2019	283.4	18.6%	40.4%	77.9	20.1%	43.5%
2020	274.5	18.2%	39.5%	77.9	20.0%	43.5%
2021	276.9	18.0%	39.1%	75.6	19.4%	42.2%

4. Limitations of the study

4.1. The present study has the following limitations:

(a) Changes in wind direction are not accounted for. In other words, the model describes the response of the wind turbines to changes in wind speed only. Changes in wind direction require the turbines to adjust their nacelle, decreasing wind generation temporarily. Our simplified approach can (at least partially) explain the relatively high capacity factors compared to previous studies[14].

(b) We modelled individual wind turbines, which could also explain the relatively high capacity factors. Wind farms are usually composed of multiple turbines and are thus subject to interference due to turbulence.

(c) We modelled the wind turbines considering a sharp cut-off in generation when wind speeds are above a certain wind speed threshold (known as cut-off speed). However, we are aware that some wind turbines have the technology to generate at higher wind speeds using a gradual de-rate curve instead of a threshold value.

(d) Solar modelling could benefit from measured solar direct normal irradiance (DNI) information. In this study, we modelled the variable, which can increase the uncertainties of the final model.

5. Conclusions

5.1. This study analysed the wind and solar behaviour at multiple locations across New Zealand, modelling the generated wind and solar power from theoretical systems. The data ranged from 2015 to 2021, recorded at hourly intervals.

[14] See, for instance: Paul Botha, Graeme Mills and Steve Harding. *Wind generation stack update.* Ministry of Business, Innovation and Employment (2020). Available at: https://www.mbie.govt.nz/assets/wind-generation-stack-update.pdf.

5.2. The study investigated the time and space variability of the wind and solar systems, to understand how generation from both sources varies in time and the spatial correlation between sites.

5.3. The study found that, for wind, 5 percent of the time generation was below 10 percent of total capacity (around 27 MW from a nominal wind generation capacity of 267 MW – or all 89 turbines operating at a nominal capacity of 3MW each), whilst 9 percent of the time generation was above 50 percent of this capacity over the entire country. When considering the islands, the North Island results showed better performance when compared to the South Island. The wind sites showed an overall tendency to generate more energy during the daytime – peaking about 4pm in spring and summer and 2 pm in winter - but had a median daily variation in spring of 79 MW. While this daily variation was lower in winter (median of 52 MW), the average wind generation in spring was 20 percent higher than in winter.

5.4. The seasonal pattern, the intraday pattern and the amount of time that utilisation is below 10 percent of capacity means that firming needs to develop along side renewable investment.

5.5. The study also found an increase in the correlation values between the sites depending on their proximity (the closer the sites, the higher the correlation).

5.6. For solar power, the study found that 60 percent of the time generation was below 10 percent of total capacity and 14 percent of the time it was above 50 percent of the overall capacity. When excluding night-time values, 20 percent of the time generation was below 10 percent and 28 percent of the time it was above 50 percent of total capacity. Similar to wind, the North Island outperformed the South, but by a smaller margin when compared to wind. The correlation between the solar sites remained high throughout the country, despite the increase in distance between the sites. Solar has a more pronounced daily variation compared to wind, which is expected due to the characteristics of this energy source. Solar is heavily affected by the change in seasons, the average solar generation in winter was 32 percent lower when compared to the average generation over the summer months (48.6 MW against 71.6 MW during summer).

5.7. The analysis of the selected (high-performance) sites in scenario two confirmed that the spatial location affects wind generation more than solar since the latter continued showing higher correlation values despite the increase in the distance between sites. For instance, for wind, the correlation values between Cape Reinga and Whangaparaoa wind sites are higher relative to Cape Reinga and Le Bons Bay sites (0.049 versus 0.57). Such differences were not observed among the solar sites.

5.8. Finally, for wind, the capacity factors increased considerably when comparing the 13 selected sites (scenario two) against the original set of 89 sites, from around 32 percent to around 53 percent. This means that the 13 top performing sites accounted for around 25 percent of the total yearly generation from all 89 sites.

5.9. Such an increase in capacity factors was not observed for the solar sites, as they showed more homogeneous performance across the sites. The 15 selected sites (scenario two) showed average capacity factor around 20 percent while the average capacity factor for all 61 sites (scenario one) was around 18 percent.

5.10. In terms of future work, it could be worthwhile to calculate the correlation between the solar and wind generators, as well as replicate the approach used in this study with different data sets, since the data used in this study presents limitations for both wind and solar analysis. It could also be worthwhile to refine the wind modelling to account for multiple turbines and the effects of turbulence and wind direction on the machines.

5.11. Finally, we reinforce that this study should not be interpreted as a feasibility study. Rather, it serves as an indication of the behaviour of solar and wind generation throughout New Zealand based on weather data available to the Authority. Thus, the wind and solar sites mentioned in the study were selected based solely on data availability (ie, existing weather stations); the technical feasibility or economic viability of the sites is completely out of the scope of the study.

Appendix A Seasonal Wind and Solar Weather Data

A.1. Figure 17 and Figure 18 show the wind speed and solar GHI relative to the season of the year. Note, however, that the number of data sources for solar and wind are different (61 weather stations for solar versus 89 for wind)

Figure 17 - Seasonal wind speed histograms

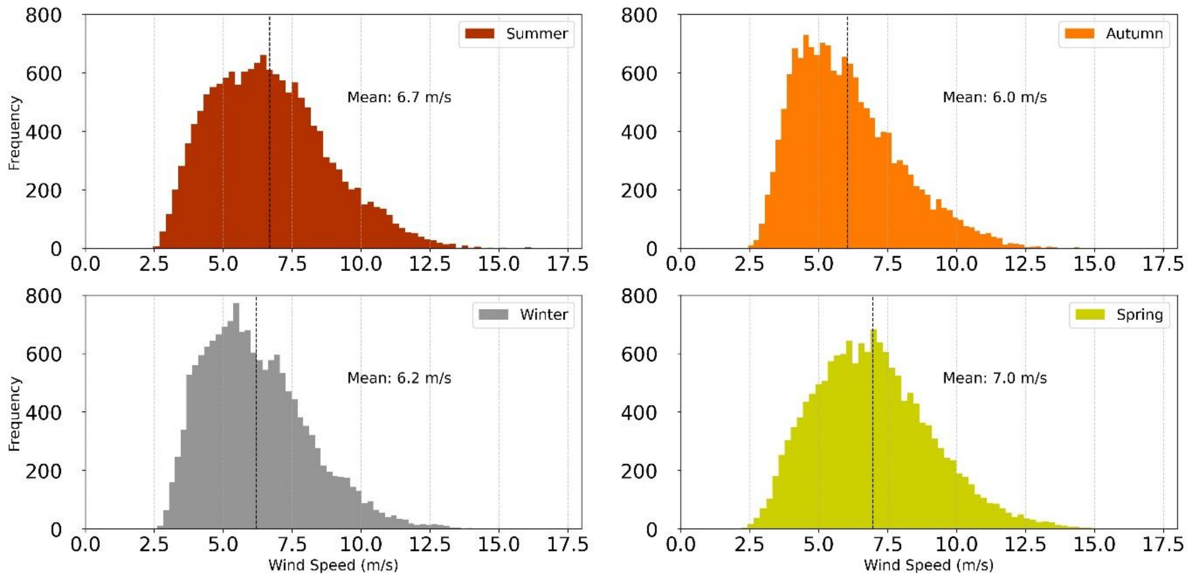

Figure 18 - Seasonal solar global horizontal irradiance (GHI) histograms

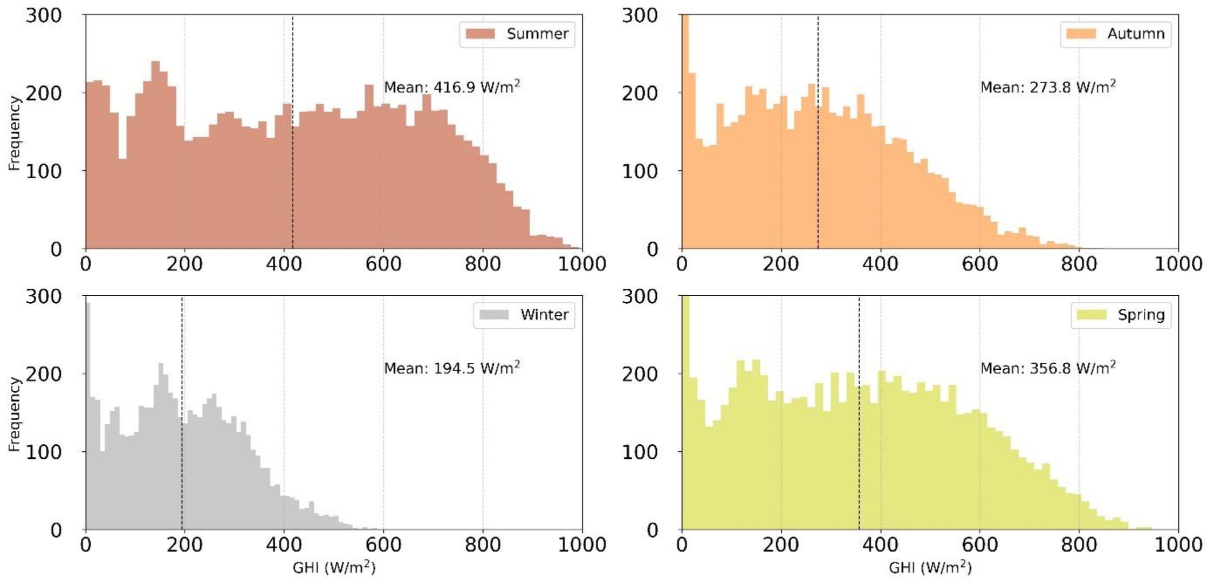

Appendix B Hourly Wind and Solar Generation Boxplots

B.1. Wind

Figure 19 - Wind Power Box plots by Month

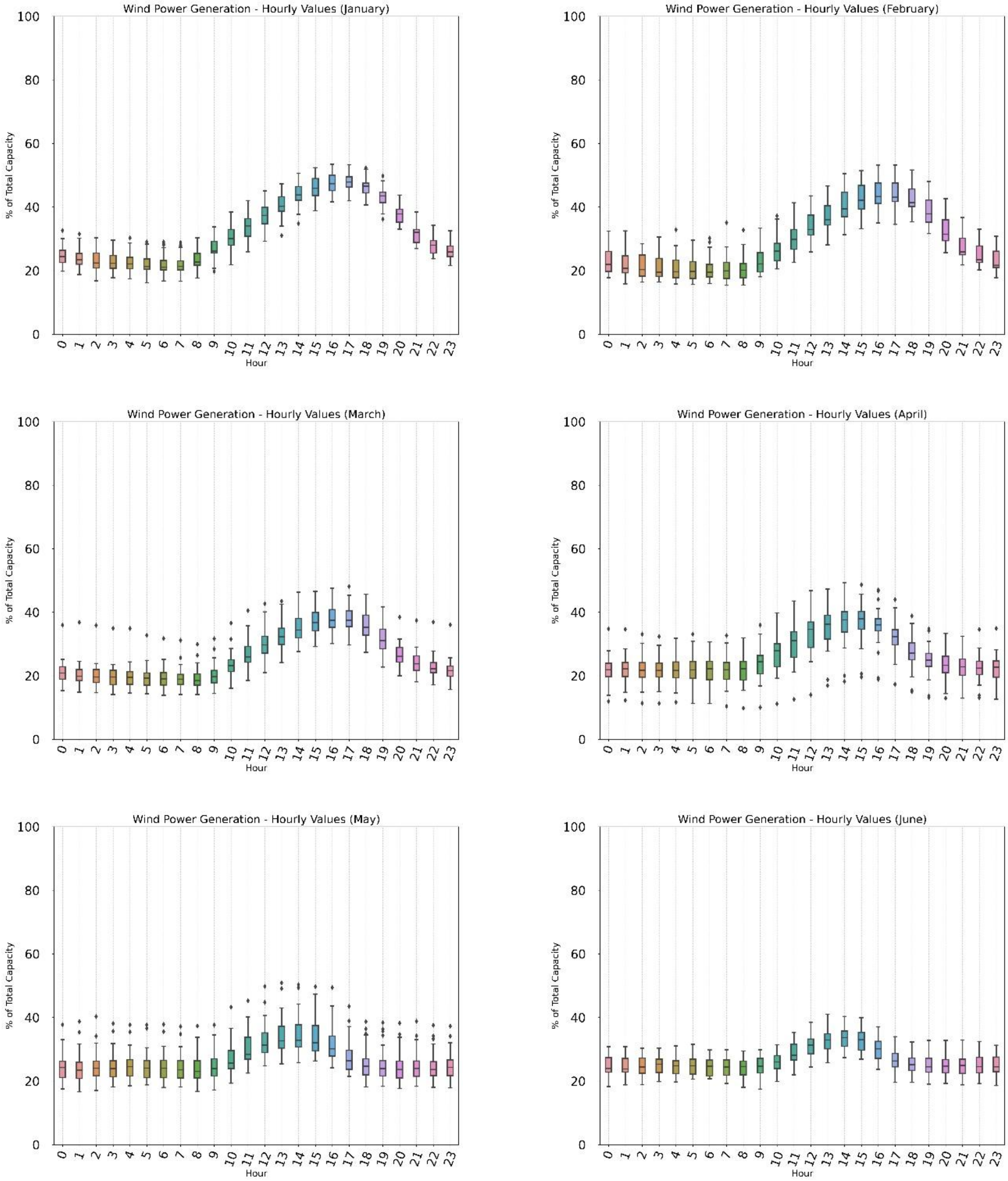

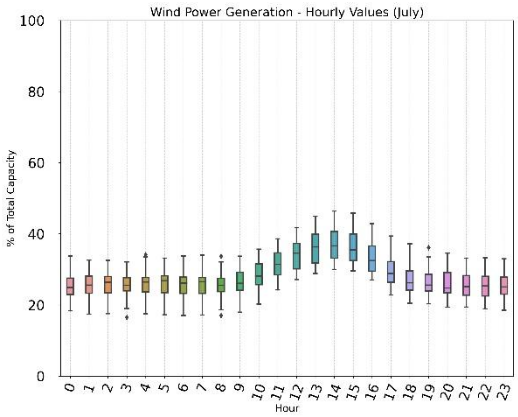
Wind Power Generation - Hourly Values (July)
% of Total Capacity
Hour

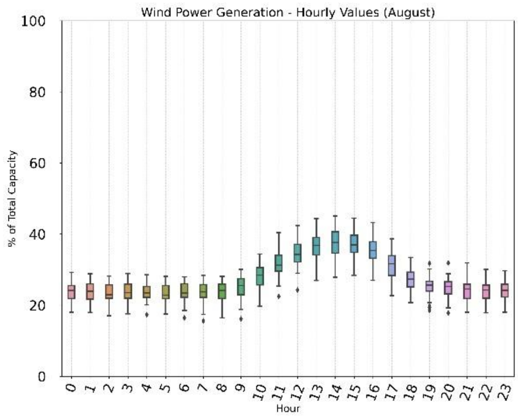
Wind Power Generation - Hourly Values (August)
% of Total Capacity
Hour

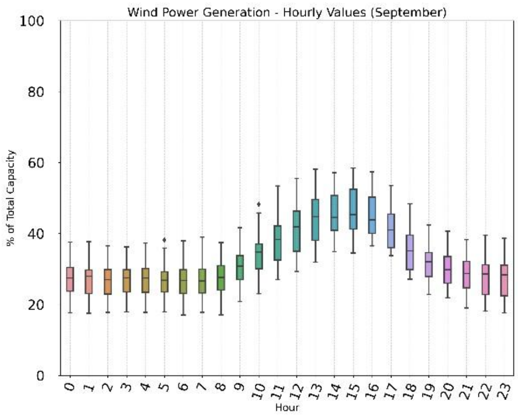
Wind Power Generation - Hourly Values (September)
% of Total Capacity
Hour

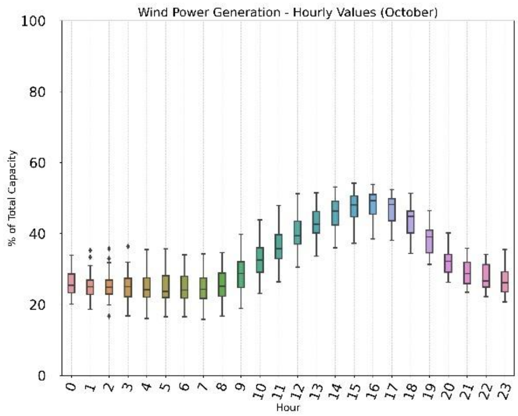
Wind Power Generation - Hourly Values (October)
% of Total Capacity
Hour

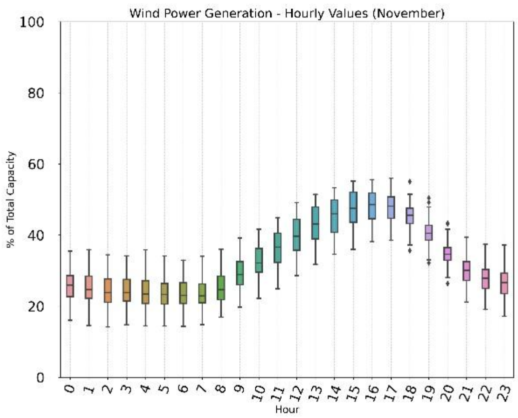
Wind Power Generation - Hourly Values (November)
% of Total Capacity
Hour

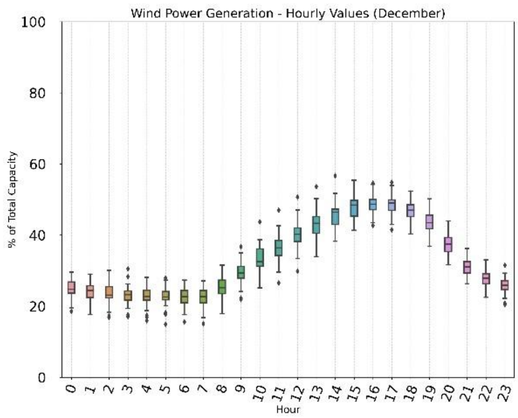
Wind Power Generation - Hourly Values (December)
% of Total Capacity
Hour

B.2. Solar

Figure 20 – Solar Power Box plots by Month

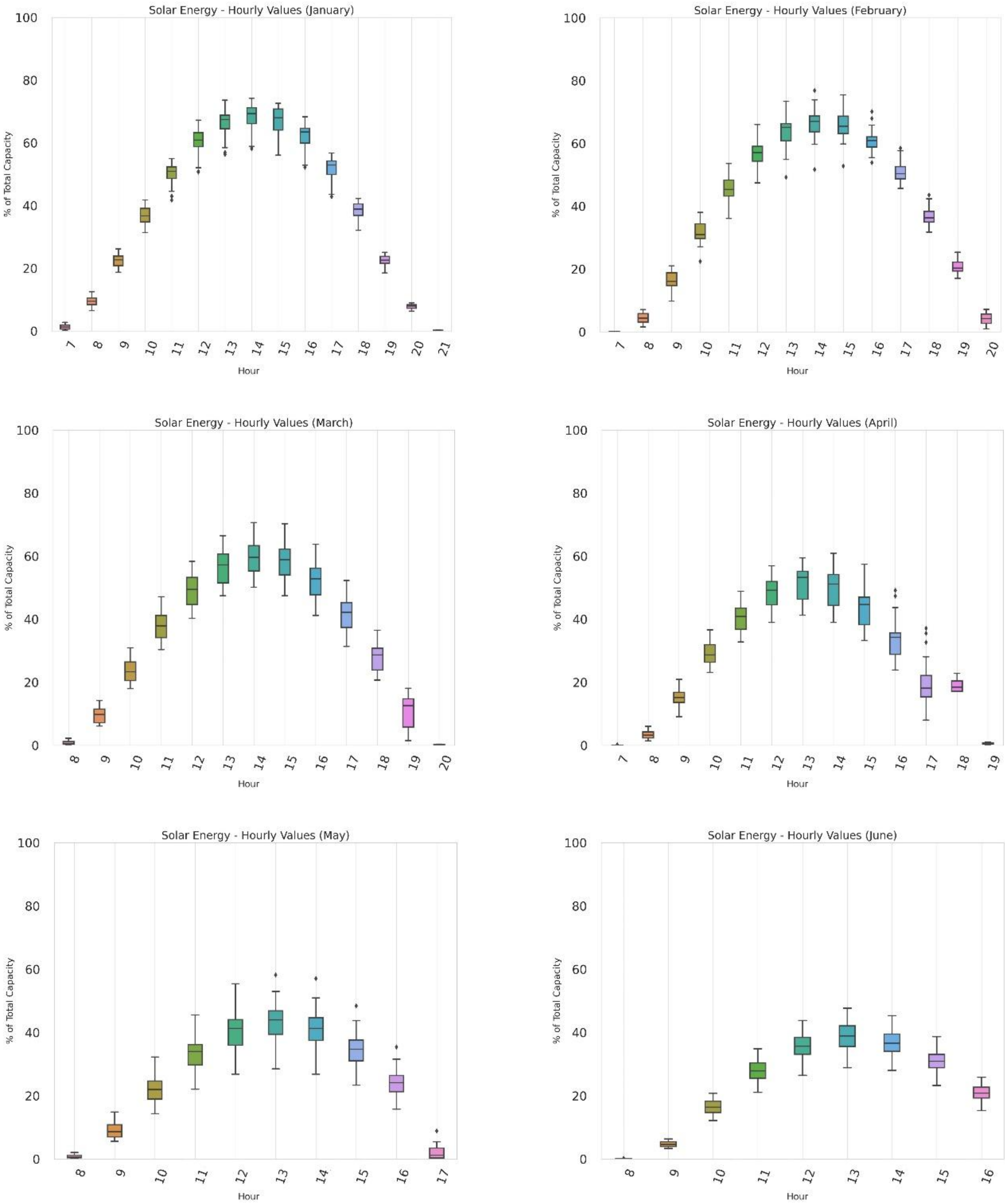

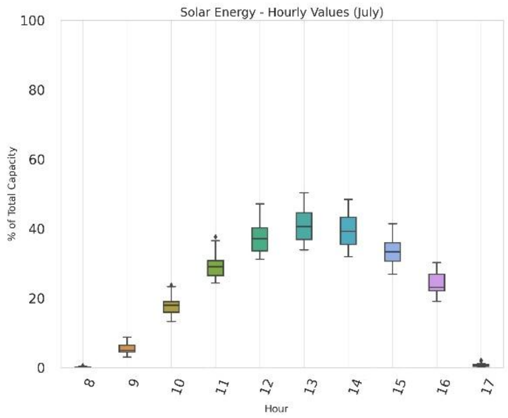
Solar Energy - Hourly Values (July)
% of Total Capacity
Hour

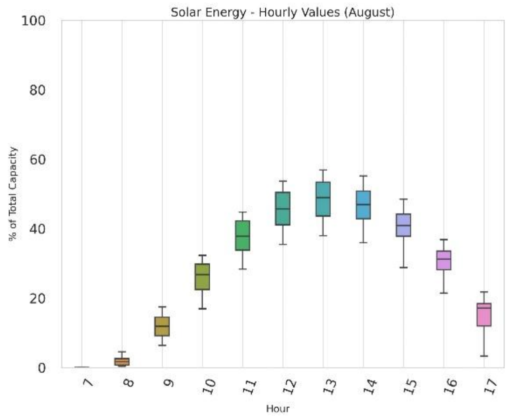
Solar Energy - Hourly Values (August)
% of Total Capacity
Hour

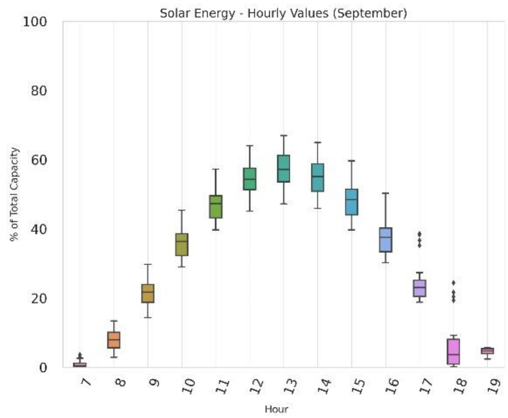
Solar Energy - Hourly Values (September)
% of Total Capacity
Hour

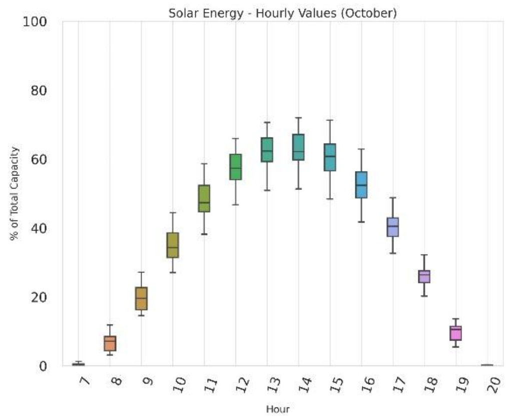
Solar Energy - Hourly Values (October)
% of Total Capacity
Hour

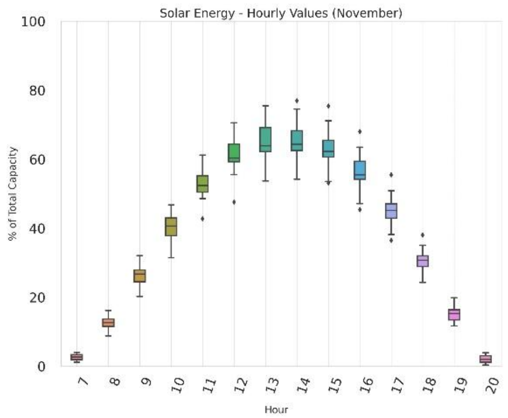
Solar Energy - Hourly Values (November)
% of Total Capacity
Hour

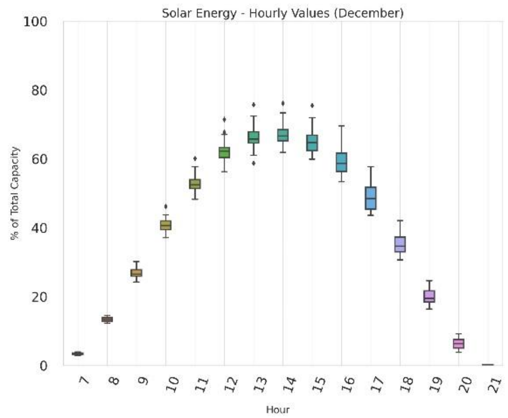
Solar Energy - Hourly Values (December)
% of Total Capacity
Hour

Appendix C Regional Analysis

C.1. Wind

Figure 21 - Left: box-and-whisker chart showing the modelled performance of wind sites for each region. Right: Correlation between the sites.

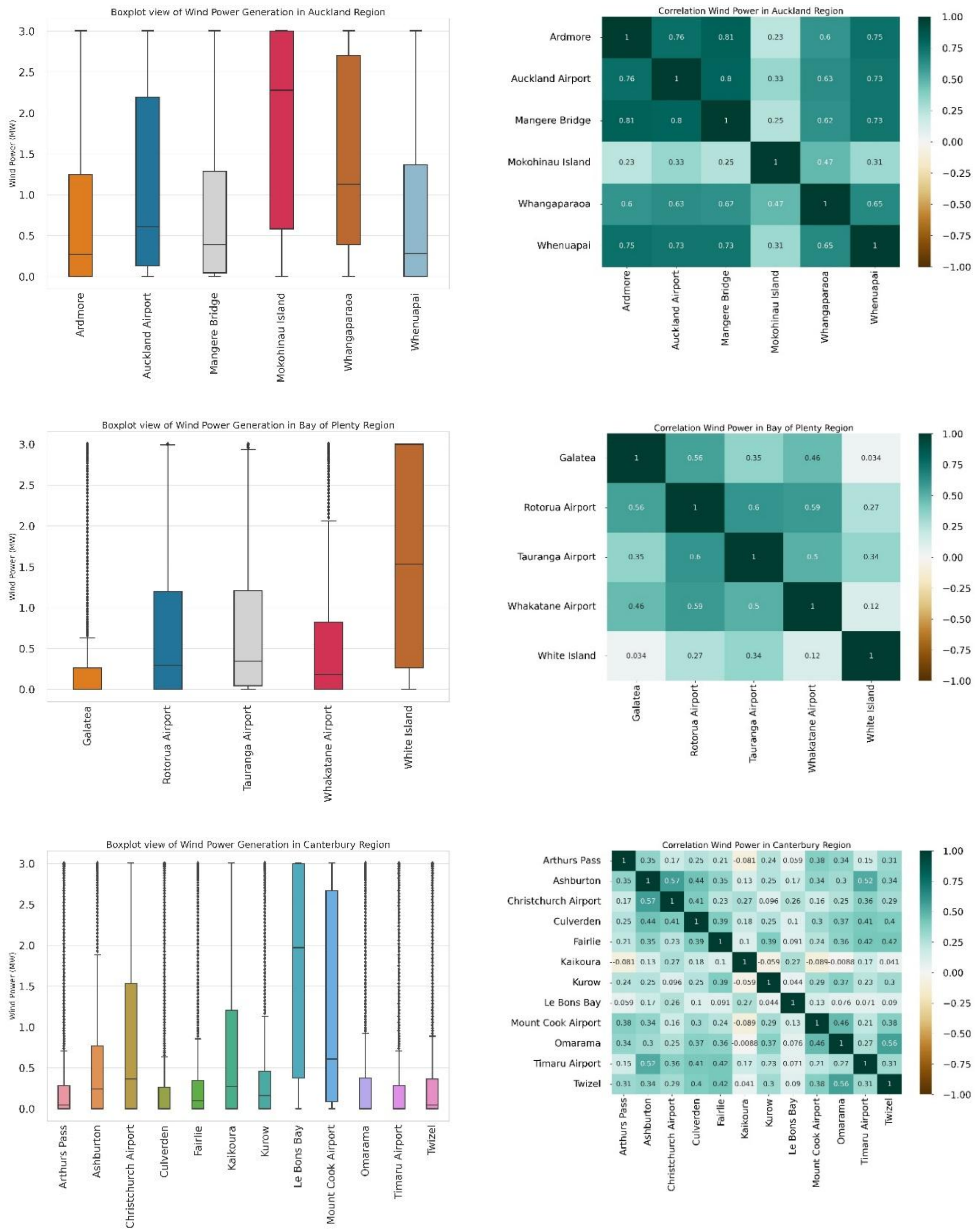

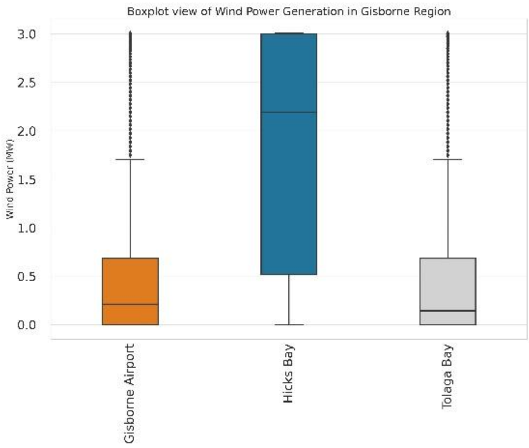
Boxplot view of Wind Power Generation in Gisborne Region
Wind Power (MW)
3.0
2.5
2.0
1.5
1.0
0.5
0.0
Gisborne Airport
Hicks Bay
Tolaga Bay

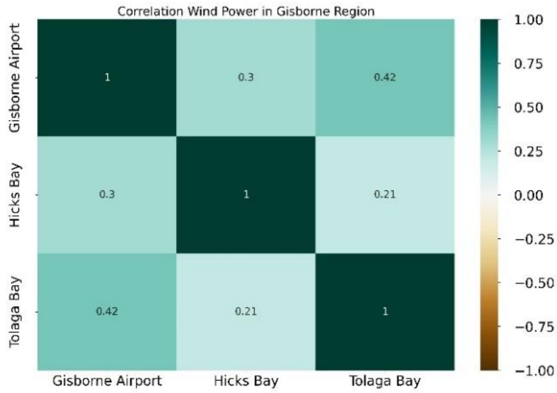
Correlation Wind Power in Gisborne Region
Gisborne Airport
Hicks Bay
Tolaga Bay
1
0.3
0.42
0.3
1
0.21
0.42
0.21
1
1.00
0.75
0.50
0.25
0.00
−0.25
−0.50
−0.75
−1.00

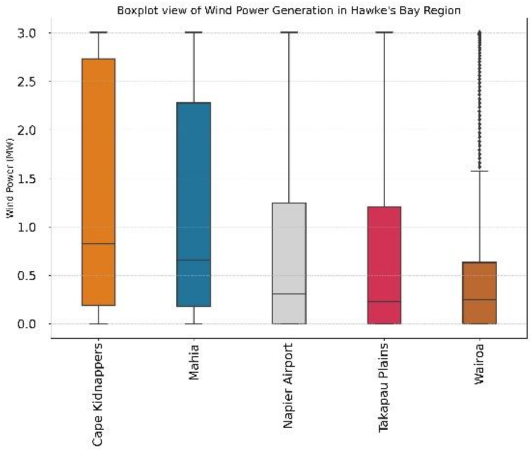
Boxplot view of Wind Power Generation in Hawke's Bay Region
Wind Power (MW)
3.0
2.5
2.0
1.5
1.0
0.5
0.0
Cape Kidnappers
Mahia
Napier Airport
Takapau Plains
Wairoa

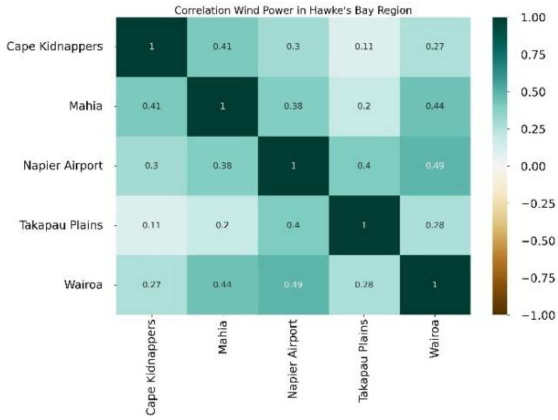
Correlation Wind Power in Hawke's Bay Region
Cape Kidnappers
Mahia
Napier Airport
Takapau Plains
Wairoa
1
0.41
0.3
0.11
0.27
0.41
1
0.38
0.2
0.44
0.3
0.38
1
0.4
0.49
0.11
0.2
0.4
1
0.28
0.27
0.44
0.49
0.28
1
1.00
0.75
0.50
0.25
0.00
−0.25
−0.50
−0.75
−1.00

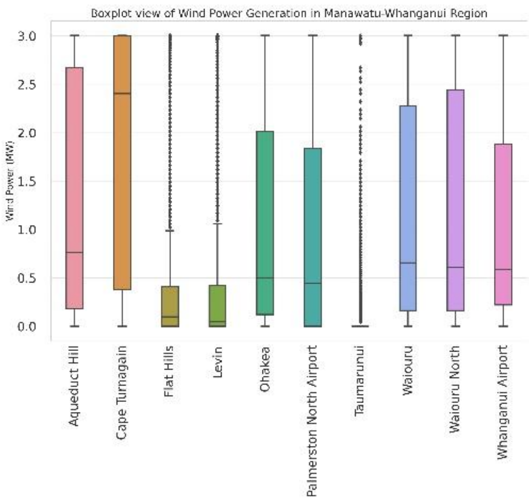
Boxplot view of Wind Power Generation in Manawatu-Whanganui Region
Wind Power (MW)
3.0
2.5
2.0
1.5
1.0
0.5
0.0
Aqueduct Hill
Cape Turnagain
Flat Hills
Levin
Ohakea
Palmerston North Airport
Taumarunui
Waiouru
Waiouru North
Whanganui Airport

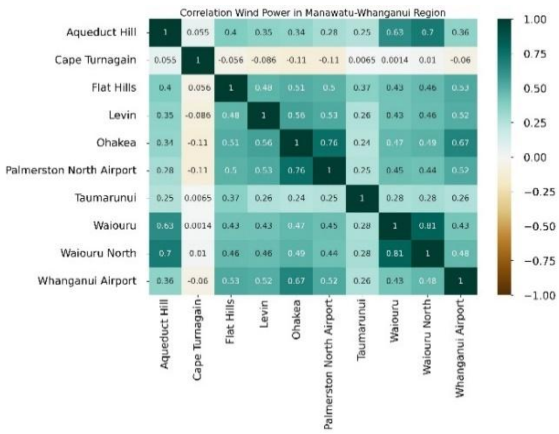
Correlation Wind Power in Manawatu-Whanganui Region
Aqueduct Hill
Cape Turnagain
Flat Hills
Levin
Ohakea
Palmerston North Airport
Taumarunui
Waiouru
Waiouru North
Whanganui Airport
1.00
0.75
0.50
0.25
0.00
−0.25
−0.50
−0.75
−1.00

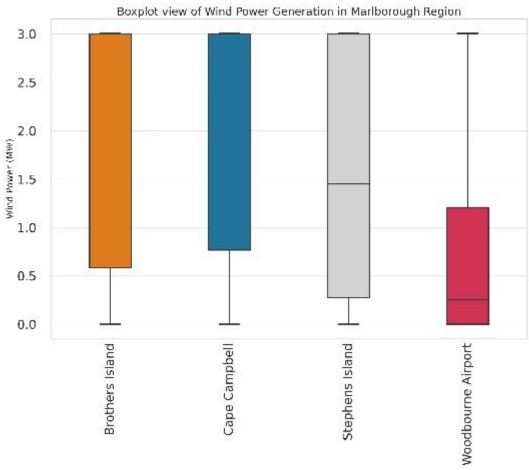
Boxplot view of Wind Power Generation in Marlborough Region
Wind Power (MW)
3.0
2.5
2.0
1.5
1.0
0.5
0.0
Brothers Island
Cape Campbell
Stephens Island
Woodbourne Airport

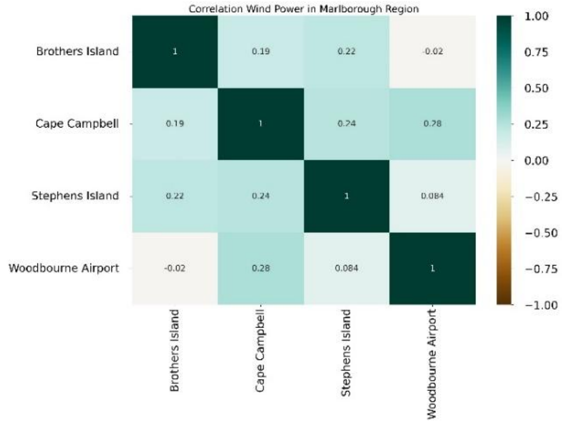
Correlation Wind Power in Marlborough Region
Brothers Island
Cape Campbell
Stephens Island
Woodbourne Airport
1 0.19 0.22 -0.02
0.19 1 0.24 0.28
0.22 0.24 1 0.084
-0.02 0.28 0.084 1
1.00
0.75
0.50
0.25
0.00
−0.25
−0.50
−0.75
−1.00

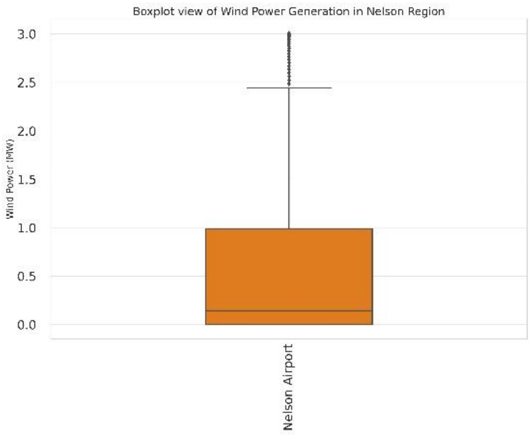
Boxplot view of Wind Power Generation in Nelson Region
Wind Power (MW)
3.0
2.5
2.0
1.5
1.0
0.5
0.0
Nelson Airport

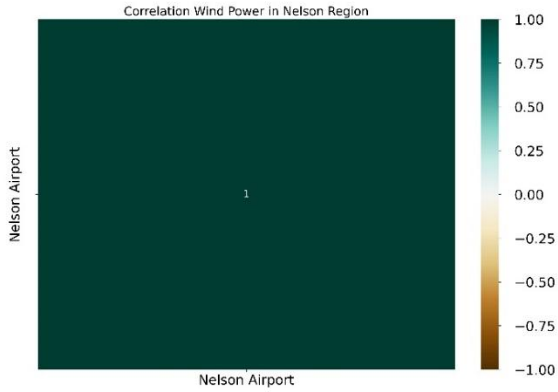
Correlation Wind Power in Nelson Region
Nelson Airport
1
Nelson Airport
1.00
0.75
0.50
0.25
0.00
−0.25
−0.50
−0.75
−1.00

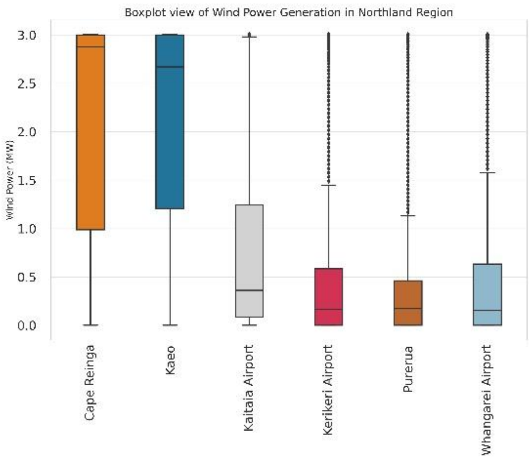
Boxplot view of Wind Power Generation in Northland Region
Wind Power (MW)
3.0
2.5
2.0
1.5
1.0
0.5
0.0
Cape Reinga
Kaeo
Kaitaia Airport
Kerikeri Airport
Purerua
Whangarei Airport

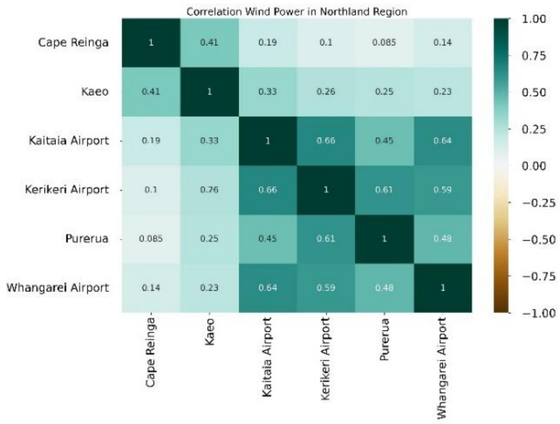
Correlation Wind Power in Northland Region
Cape Reinga
Kaeo
Kaitaia Airport
Kerikeri Airport
Purerua
Whangarei Airport
1 0.41 0.19 0.1 0.085 0.14
0.41 1 0.33 0.26 0.25 0.23
0.19 0.33 1 0.66 0.45 0.64
0.1 0.26 0.66 1 0.61 0.59
0.085 0.25 0.45 0.61 1 0.48
0.14 0.23 0.64 0.59 0.48 1
1.00
0.75
0.50
0.25
0.00
−0.25
−0.50
−0.75
−1.00

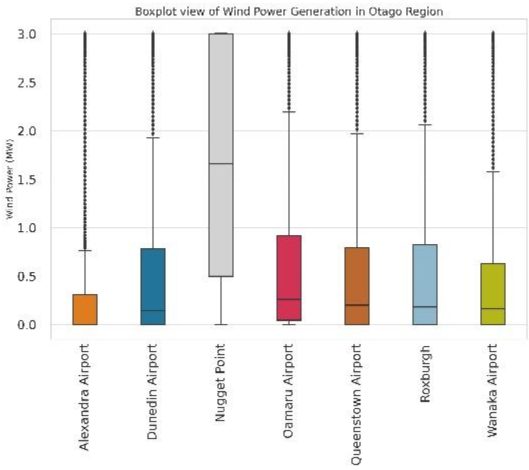
Boxplot view of Wind Power Generation in Otago Region
Wind Power (MW)
3.0
2.5
2.0
1.5
1.0
0.5
0.0
Alexandra Airport
Dunedin Airport
Nugget Point
Oamaru Airport
Queenstown Airport
Roxburgh
Wanaka Airport

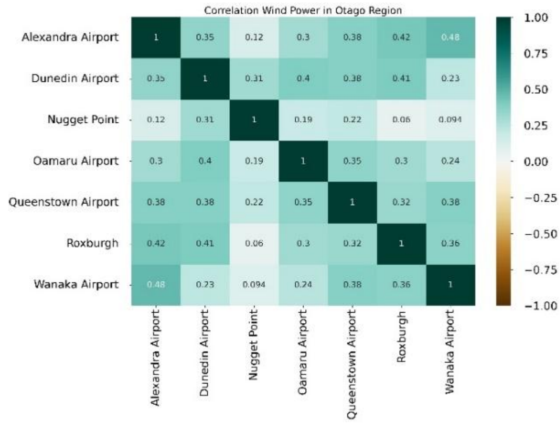
Correlation Wind Power in Otago Region
Alexandra Airport
Dunedin Airport
Nugget Point
Oamaru Airport
Queenstown Airport
Roxburgh
Wanaka Airport
1 0.35 0.12 0.3 0.38 0.42 0.48
0.35 1 0.31 0.4 0.38 0.41 0.23
0.12 0.31 1 0.19 0.22 0.06 0.094
0.3 0.4 0.19 1 0.35 0.3 0.24
0.38 0.38 0.22 0.35 1 0.32 0.38
0.42 0.41 0.06 0.3 0.32 1 0.36
0.48 0.23 0.094 0.24 0.38 0.36 1
1.00
0.75
0.50
0.25
0.00
−0.25
−0.50
−0.75
−1.00

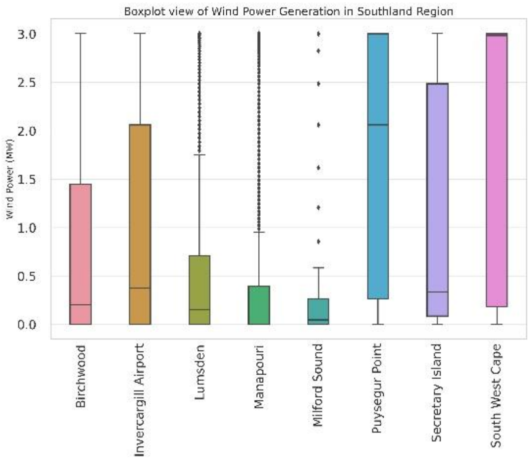
Boxplot view of Wind Power Generation in Southland Region
Wind Power (MW)
3.0
2.5
2.0
1.5
1.0
0.5
0.0
Birchwood
Invercargill Airport
Lumsden
Manapouri
Milford Sound
Puysegur Point
Secretary Island
South West Cape

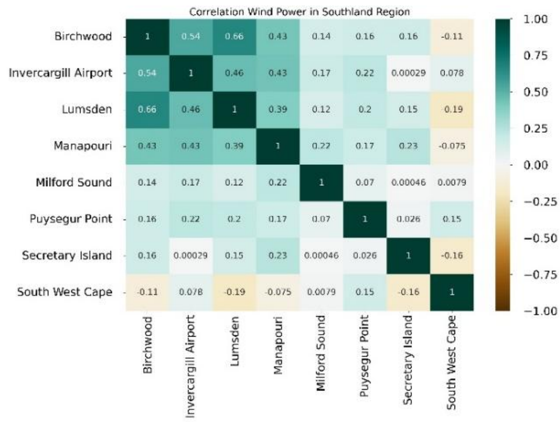
Correlation Wind Power in Southland Region
Birchwood
Invercargill Airport
Lumsden
Manapouri
Milford Sound
Puysegur Point
Secretary Island
South West Cape
1 0.54 0.66 0.43 0.14 0.16 0.16 -0.11
0.54 1 0.46 0.43 0.17 0.22 0.00029 0.078
0.66 0.46 1 0.39 0.12 0.2 0.15 0.19
0.43 0.43 0.39 1 0.22 0.17 0.23 -0.075
0.14 0.17 0.12 0.22 1 0.07 0.00046 0.0079
0.16 0.22 0.2 0.17 0.07 1 0.026 0.15
0.16 0.00029 0.15 0.23 0.00046 0.026 1 -0.16
-0.11 0.078 -0.19 -0.075 0.0079 0.15 -0.16 1
1.00
0.75
0.50
0.25
0.00
−0.25
−0.50
−0.75
−1.00

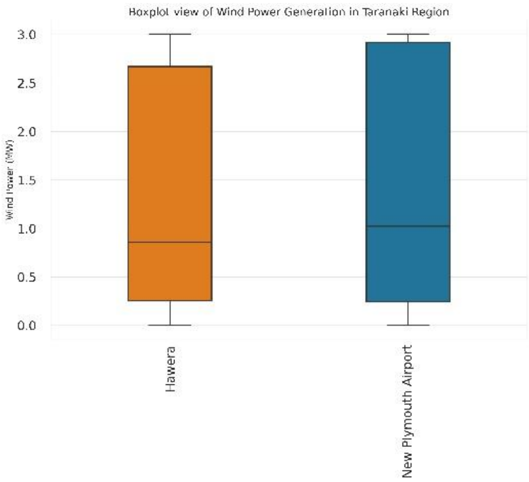
Boxplot view of Wind Power Generation in Taranaki Region
Wind Power (MW)
3.0
2.5
2.0
1.5
1.0
0.5
0.0
Hawera
New Plymouth Airport

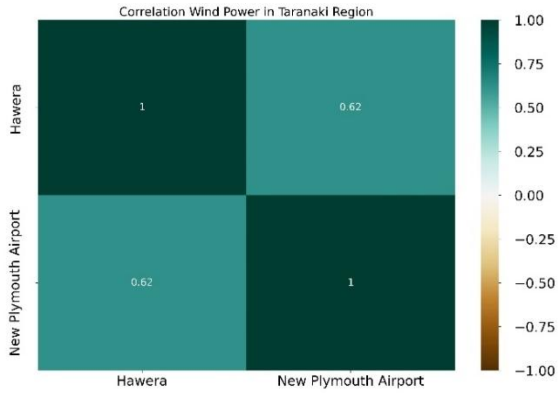
Correlation Wind Power in Taranaki Region
Hawera
New Plymouth Airport
1 0.62
0.62 1
Hawera
New Plymouth Airport
1.00
0.75
0.50
0.25
0.00
−0.25
−0.50
−0.75
−1.00

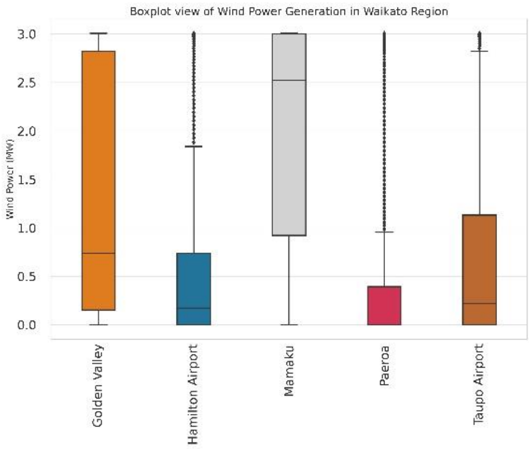
Boxplot view of Wind Power Generation in Waikato Region
Wind Power (MW)
3.0
2.5
2.0
1.5
1.0
0.5
0.0
Golden Valley
Hamilton Airport
Mamaku
Paeroa
Taupo Airport

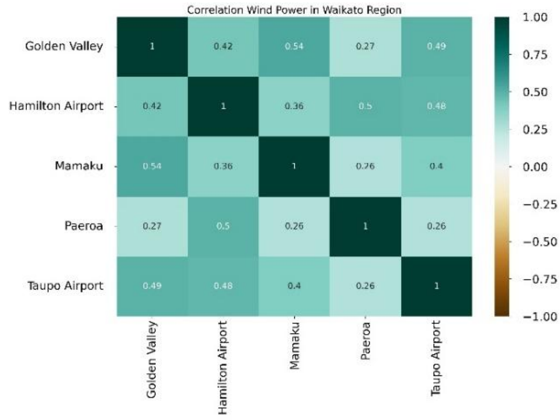
Correlation Wind Power in Waikato Region
Golden Valley
Hamilton Airport
Mamaku
Paeroa
Taupo Airport
1.00
0.75
0.50
0.25
0.00
−0.25
−0.50
−0.75
−1.00

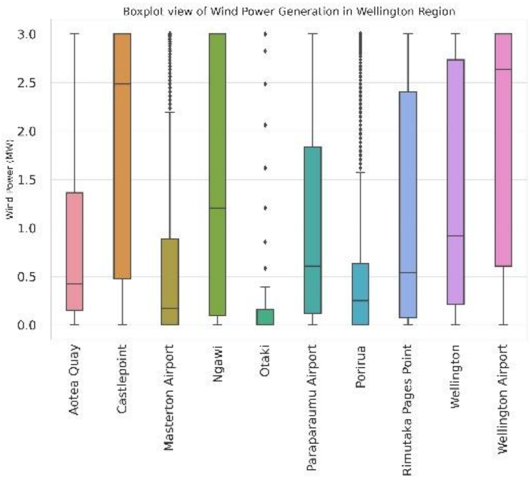
Boxplot view of Wind Power Generation in Wellington Region
Wind Power (MW)
3.0
2.5
2.0
1.5
1.0
0.5
0.0
Aotea Quay
Castlepoint
Masterton Airport
Ngawi
Otaki
Paraparaumu Airport
Porirua
Rimutaka Pages Point
Wellington
Wellington Airport

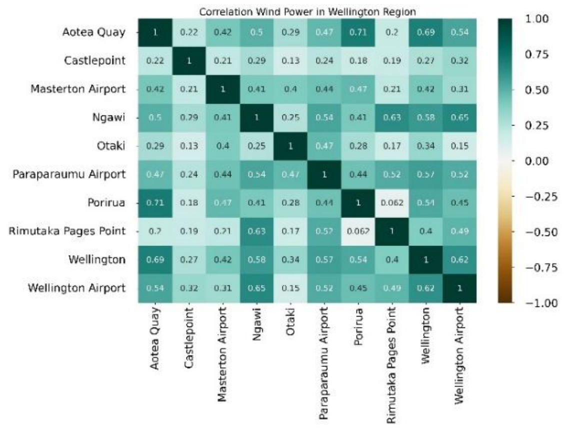
Correlation Wind Power in Wellington Region
Aotea Quay
Castlepoint
Masterton Airport
Ngawi
Otaki
Paraparaumu Airport
Porirua
Rimutaka Pages Point
Wellington
Wellington Airport
1.00
0.75
0.50
0.25
0.00
−0.25
−0.50
−0.75
−1.00

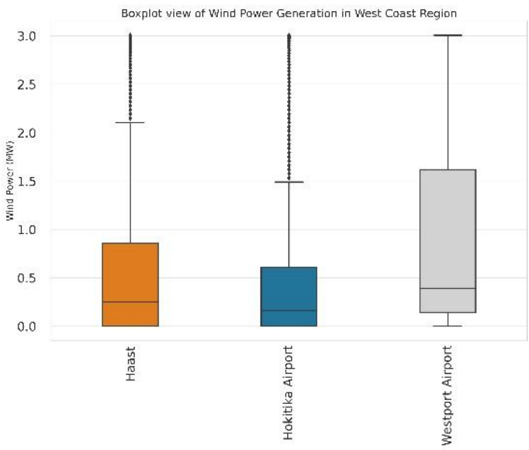
Boxplot view of Wind Power Generation in West Coast Region
Wind Power (MW)
3.0
2.5
2.0
1.5
1.0
0.5
0.0
Haast
Hokitika Airport
Westport Airport

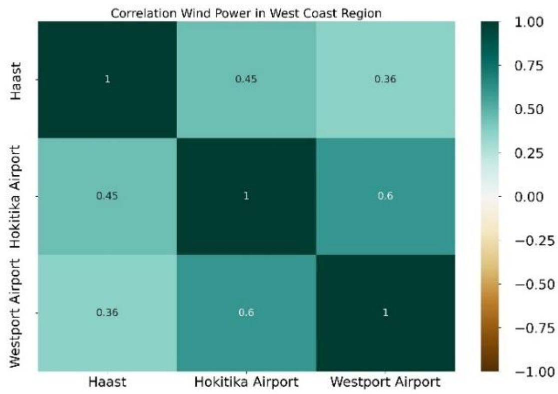
Correlation Wind Power in West Coast Region
Haast
Hokitika Airport
Westport Airport
1.00
0.75
0.50
0.25
0.00
−0.25
−0.50
−0.75
−1.00

A.1 Solar

Figure 22 - - Left: box-and-whisker chart showing the modelled performance of solar sites for each region. Right: Correlation between the sites

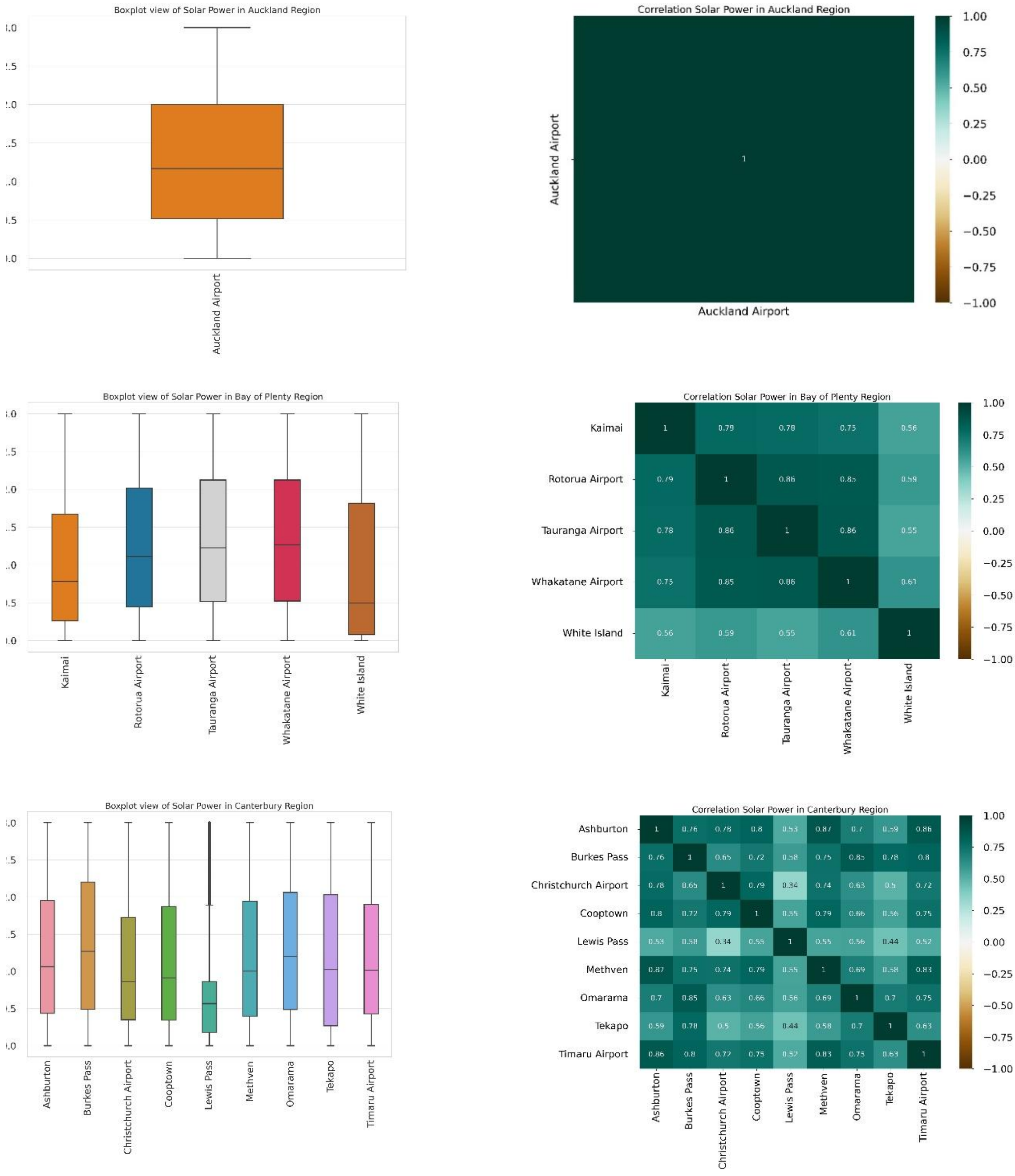

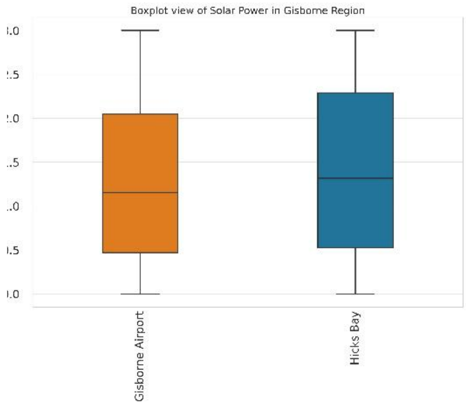
Boxplot view of Solar Power in Gisborne Region
Gisborne Airport
Hicks Bay

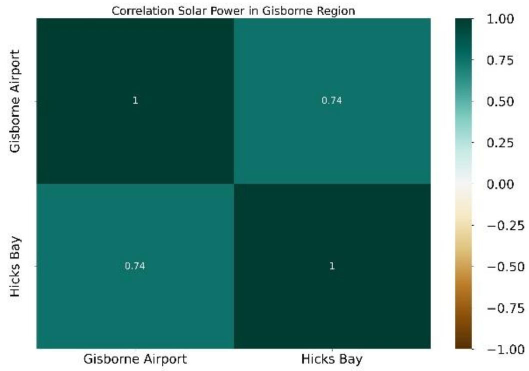
Correlation Solar Power in Gisborne Region
Gisborne Airport
Hicks Bay

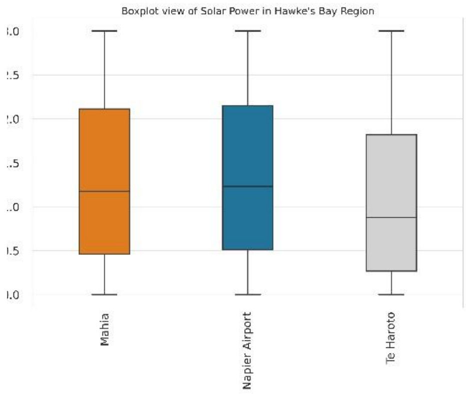
Boxplot view of Solar Power in Hawke's Bay Region
Mahia
Napier Airport
Te Haroto

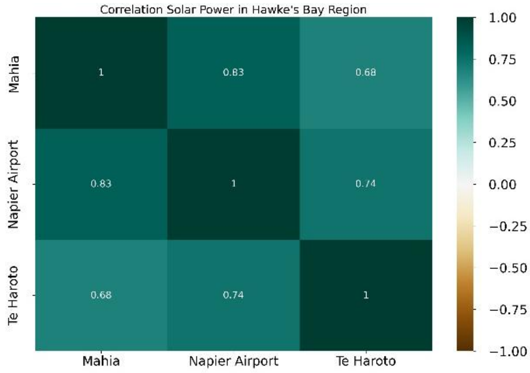
Correlation Solar Power in Hawke's Bay Region
Mahia
Napier Airport
Te Haroto

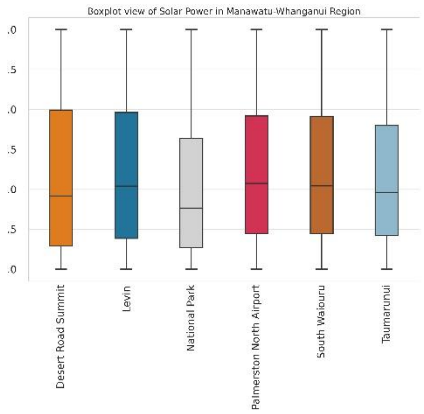
Boxplot view of Solar Power in Manawatu-Whanganui Region
Desert Road Summit
Levin
National Park
Palmerston North Airport
South Waiouru
Taumarunui

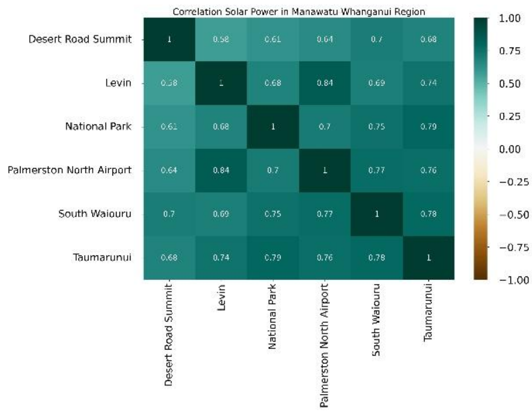
Correlation Solar Power in Manawatu Whanganui Region
Desert Road Summit
Levin
National Park
Palmerston North Airport
South Waiouru
Taumarunui

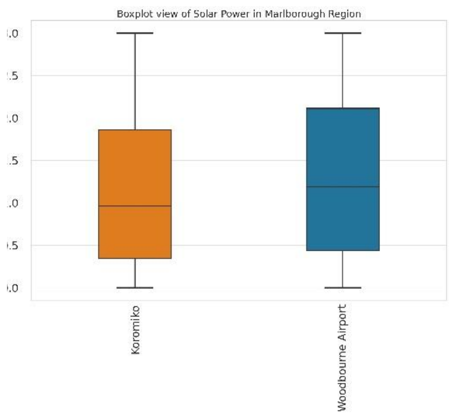
Boxplot view of Solar Power in Marlborough Region
Koromiko
Woodbourne Airport


Correlation Solar Power in Marlborough Region
Koromiko
Woodbourne Airport

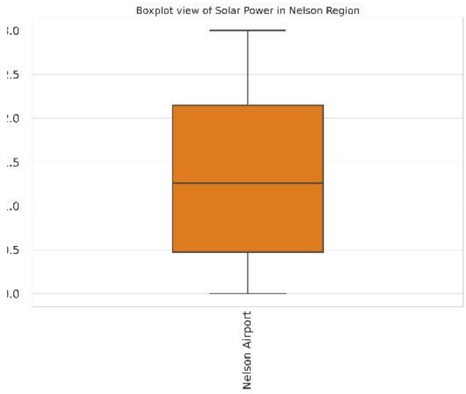
Boxplot view of Solar Power in Nelson Region
Nelson Airport

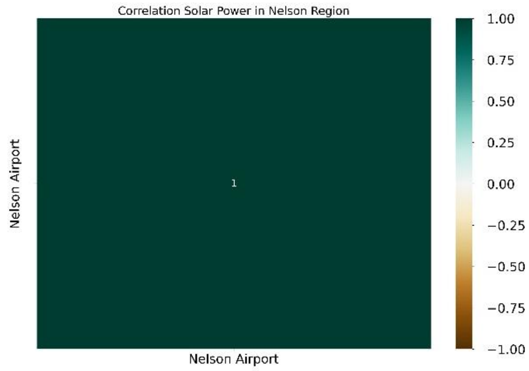
Correlation Solar Power in Nelson Region
Nelson Airport
1
Nelson Airport
1.00
0.75
0.50
0.25
0.00
−0.25
−0.50
−0.75
−1.00

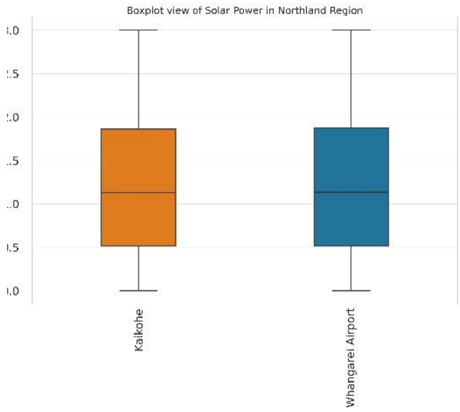
Boxplot view of Solar Power in Northland Region
Kaikohe
Whangarei Airport

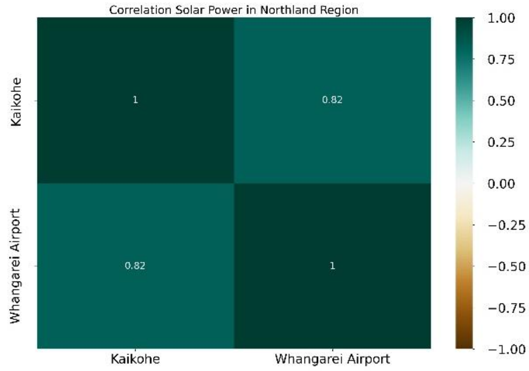
Correlation Solar Power in Northland Region
Kaikohe
Whangarei Airport
1
0.82
0.82
1
Kaikohe
Whangarei Airport
1.00
0.75
0.50
0.25
0.00
−0.25
−0.50
−0.75
−1.00

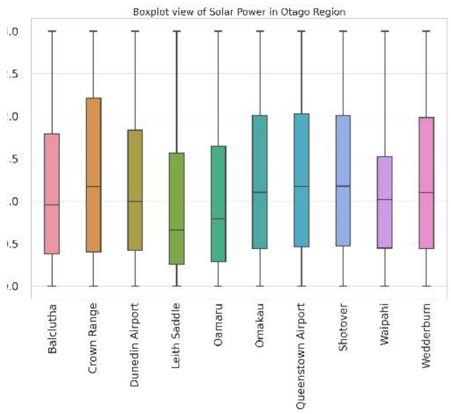
Boxplot view of Solar Power in Otago Region
Balclutha
Crown Range
Dunedin Airport
Leith Saddle
Oamaru
Omakau
Queenstown Airport
Shotover
Waipahi
Wedderburn

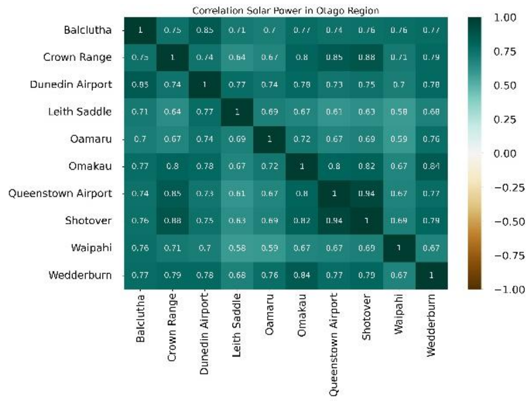
Correlation Solar Power in Otago Region
Balclutha
Crown Range
Dunedin Airport
Leith Saddle
Oamaru
Omakau
Queenstown Airport
Shotover
Waipahi
Wedderburn
1.00
0.75
0.50
0.25
0.00
−0.25
−0.50
−0.75
−1.00

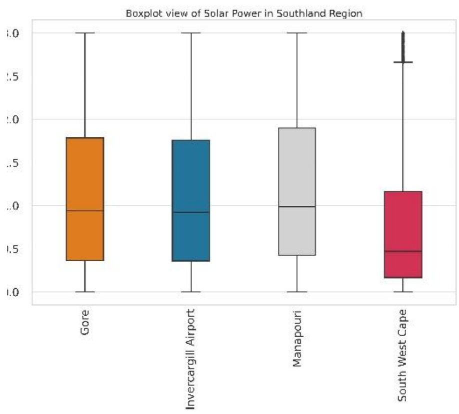
Boxplot view of Solar Power in Southland Region
Gore
Invercargill Airport
Manapouri
South West Cape

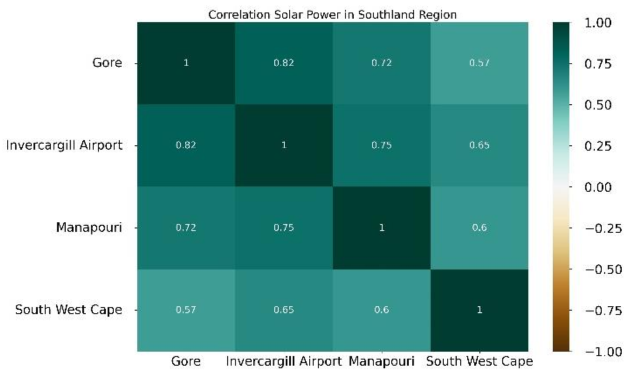
Correlation Solar Power in Southland Region
Gore
Invercargill Airport
Manapouri
South West Cape
1
0.82
0.72
0.57
0.82
1
0.75
0.65
0.72
0.75
1
0.6
0.57
0.65
0.6
1
Gore
Invercargill Airport
Manapouri
South West Cape
1.00
0.75
0.50
0.25
0.00
−0.25
−0.50
−0.75
−1.00

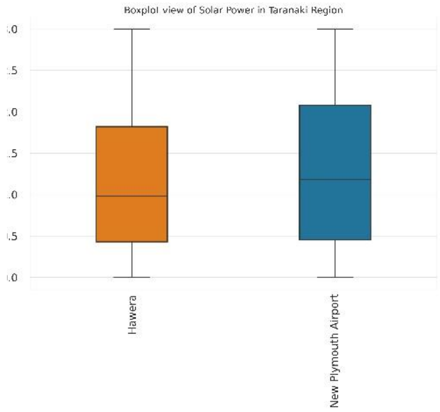
Boxplot view of Solar Power in Taranaki Region
Hawera
New Plymouth Airport

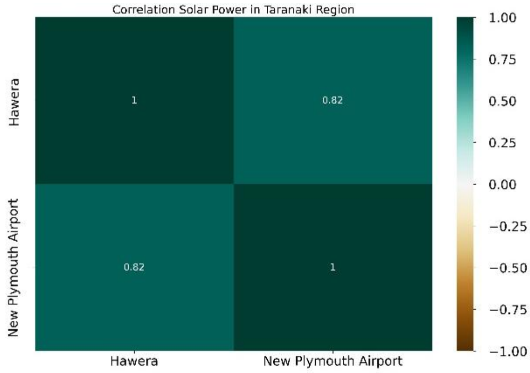
Correlation Solar Power in Taranaki Region
Hawera
New Plymouth Airport
1
0.82
0.82
1
Hawera
New Plymouth Airport
1.00
0.75
0.50
0.25
0.00
−0.25
−0.50
−0.75
−1.00

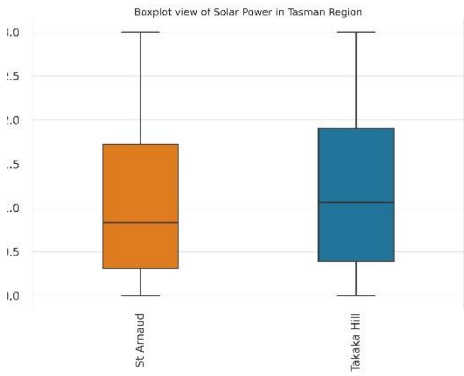
Boxplot view of Solar Power in Tasman Region
St Arnaud
Takaka Hill

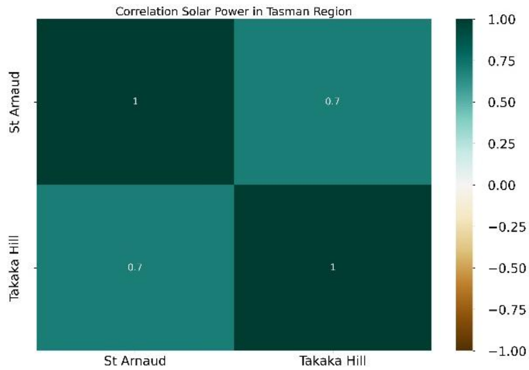
Correlation Solar Power in Tasman Region
St Arnaud
Takaka Hill
1
0.7
0.7
1
St Arnaud
Takaka Hill
1.00
0.75
0.50
0.25
0.00
−0.25
−0.50
−0.75
−1.00

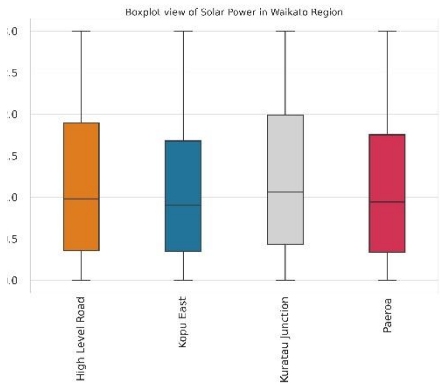
Boxplot view of Solar Power in Waikato Region
High Level Road
Kopu East
Kuratau Junction
Paeroa

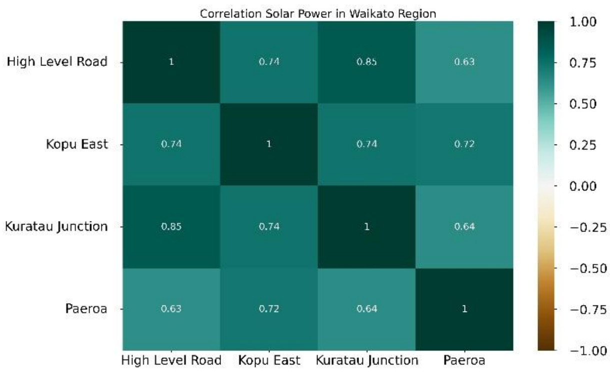
Correlation Solar Power in Waikato Region
High Level Road
1
0.74
0.85
0.63
Kopu East
0.74
1
0.74
0.72
Kuratau Junction
0.85
0.74
1
0.64
Paeroa
0.63
0.72
0.64
1
High Level Road
Kopu East
Kuratau Junction
Paeroa
1.00
0.75
0.50
0.25
0.00
−0.25
−0.50
−0.75
−1.00

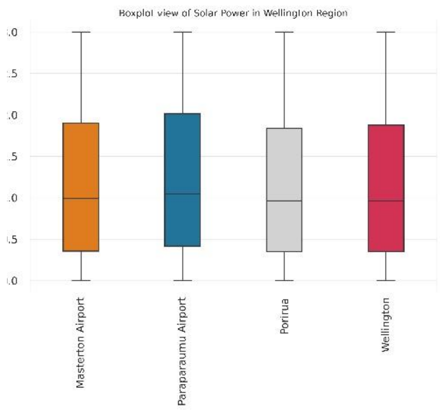
Boxplot view of Solar Power in Wellington Region
Masterton Airport
Paraparaumu Airport
Porirua
Wellington

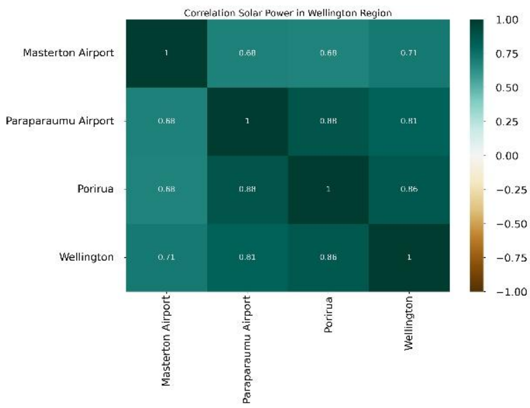
Correlation Solar Power in Wellington Region
Masterton Airport
Paraparaumu Airport
Porirua
Wellington
Masterton Airport
Paraparaumu Airport
Porirua
Wellington
1.00
0.75
0.50
0.25
0.00
−0.25
−0.50
−0.75
−1.00

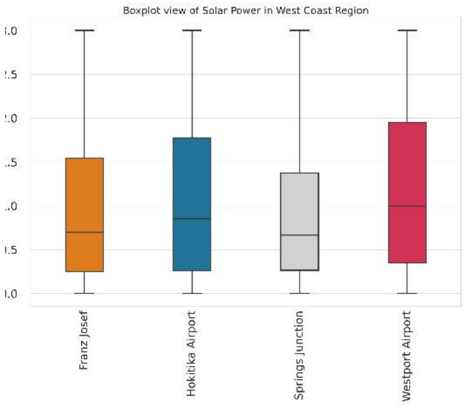

Boxplot view of Solar Power in West Coast Region
Franz Josef
Hokitika Airport
Springs Junction
Westport Airport

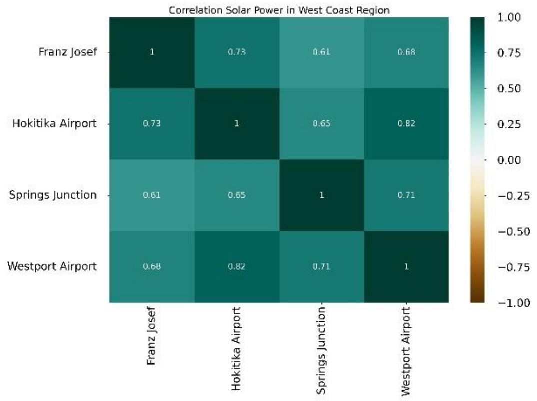

Correlation Solar Power in West Coast Region
Franz Josef
Hokitika Airport
Springs Junction
Westport Airport
1
0.73
0.61
0.68
0.65
0.82
0.71
1.00
0.75
0.50
0.25
0.00
−0.25
−0.50
−0.75
−1.00

Appendix D No Wind Generation per Site

D.1. Table 3 shows the number of occurrences when there is no wind generation for each of the 89 weather stations used in this study (sorted in alphabetical order). The values represent the percent of time each station was above or below the wind generation cut-in and cut-off thresholds. On average wind speed was below the cut-in 25.7 percent of the time, considering all the 89 stations, with a standard deviation of 16.7 percent. The average cut-off occurrence was 0.7 percent, with a standard deviation of 2 percent. Shaded rows represent the selected (top-performing) sites used in scenario two.

Table 3 - List of stations used in the study showing their respective performance relative to wind generation thresholds (cut-in and cut-off).

Station Name	Below Cut-in (%)	Above Cut-off (%)
Alexandra Airport	54.41	0.01
Aotea Quay	14.75	0
Aqueduct Hill	14.98	0.11
Ardmore	30.71	0
Arthurs Pass	48.56	0
Ashburton	2.85	0
Auckland Airport	19.62	0.01
Auckland Harbour Bridge	14.15	0.06
Birchwood	34.66	0.14
Brothers Island	4.06	10.12
Cape Campbell	5.57	1.25
Cape Kidnappers	13.16	0.72
Cape Reinga	2.5	4.22
Cape Turnagain	2.77	10.77
Castlepoint	4.76	7.38
Christchurch Airport	27.06	0.01
Culverden	57.64	0
Dunedin Airport	42.99	0.03
Fairlie	42.08	0.04
Flat Hills	26.74	0
Galatea	57.29	0
Gisborne Airport	33.55	0
Golden Valley	17.56	0.69

Station Name	Below Cut-in (%)	Above Cut-off (%)
Haast	29.91	0
Hamilton Airport	37.25	0
Hawera	11.52	0.04
Hicks Bay	5.17	0.81
Hokitika Airport	36.07	0.01
Invercargill Airport	24.58	0.15
Kaeo	1.71	1.3
Kaikoura	24.79	0.41
Kaitaia Airport	20.76	0
Kerikeri Airport	36.09	0
Kurow	21.75	0
Le Bons Bay	8.34	3.66
Levin	49.96	0
Lumsden	41.76	0
Mahia	15.03	0.06
Mamaku	2.19	0.81
Manapouri	52.8	0
Mangere Bridge	24.44	0
Masterton Airport	38.21	0.02
Milford Sound	44.03	0
Mokohinau Island	5.03	1.65
Mount Cook Airport	22.34	0.27
Napier Airport	29.89	0.01
Nelson Airport	42.87	0.03
New Brighton	13.99	0.01
New Plymouth Airport	10.4	0.12
Ngawi	22.02	0.05
Nugget Point	5.6	2.44
Oamaru Airport	25.01	0
Ohakea	18.86	0
Omarama	53.53	0.02
Otaki	24.47	0

Station Name	Below Cut-in (%)	Above Cut-off (%)
Paeroa	50.3	0.01
Palmerston North Airport	25.92	0
Paraparaumu Airport	20.37	0
Porirua	19.64	0
Purerua	32.33	0
Puysegur Point	8.75	6.01
Queenstown Airport	31.09	0
Rimutaka Pages Point	22.26	0.01
Rotorua Airport	30.12	0
Roxburgh	35.65	0.02
Secretary Island	10.18	0.17
South West Cape	2.17	7.23
Stephens Island	3.26	1.33
Takapau Plains	39.15	0.14
Taumarunui	84.51	0
Taupo Airport	34.22	0
Tauranga Airport	25.03	0
Timaru Airport	50.5	0
Tolaga Bay	42.28	0.01
Twizel	46.96	0.01
Waiouru	16.03	0.24
Waiouru North	15.98	0.02
Wairoa	28.18	0
Wanaka Airport	36.67	0
Wellington	15.13	0.05
Wellington Airport	8.56	0.54
Westport Airport	15.59	0.08
Whakatane Airport	38.01	0
Whanganui Airport	9.99	0.04
Whangaparaoa	4.9	0.16
Whangarei Airport	42.4	0
Whenuapai	29.05	0

Station Name	Below Cut-in (%)	Above Cut-off (%)
White Island	4.41	0.42
Woodbourne Airport	31.35	0